PONTIFÍCIA UNIVERSIDADE CATÓLICA DO RIO GRANDE DO SUL
FACULDADE DE MEDICINA
PROGRAMA DE PÓS-GRADUAÇÃO EM MEDICINA E CIÊNCIAS DA SAÚDE

RAFAEL ANDRADE CACERES

Estudo estrutural da enzima purina nucleosídeo fosforilase (E.C. 2.4.2.1) de *Mycobacterium tuberculosis*

Porto Alegre
2011

RAFAEL ANDRADE CACERES

Estudo estrutural da enzima purina nucleosídeo fosforilase (E.C. 2.4.2.1) de *Mycobacterium tuberculosis*

Tese apresentada como requisito para a obtenção do grau de Doutor pelo Programa de Pós-Graduação em Medicina e Ciências da Saúde da Pontifícia Universidade Católica do Rio Grande do Sul.

Orientador: **Prof. Dr. Walter Filgueira de Azevedo Junior**

Porto Alegre
2011

RAFAEL ANDRADE CACERES

Estudo estrutural da enzima purina nucleosídeo fosforilase (E.C. 2.4.2.1) de *Mycobacterium tuberculosis*

Tese apresentada como requisito para a obtenção do grau de Doutor pelo Programa de Pós-Graduação em Medicina e Ciências da Saúde da Pontifícia Universidade Católica do Rio Grande do Sul.

Aprovada em:_____de_____de_____.

BANCA EXAMINADORA:

_____
Dr. André Arigony Souto - PUCRS

_____
Dr. Hermes Luís Neubauer de Amorim - ULBRA

_____
Dr. Luis Augusto Basso - PUCRS

_____
Dr. Osmar Norberto de Souza - PUCRS

Porto Alegre
2011

Dedico este trabalho à minha mãe, Vera Maria Andrade, exército de um homem só, mulher de coragem, honra e determinação, que fez os meus sonhos os dela. Exemplo de caráter, perseverança e bondade. A você mãe, por todas as dificuldades, privações e também as inúmeras alegrias que vivenciamos juntos, te ofereço mais esta conquista como uma ínfima parcela de minha admiração e gratidão.

Science demands nothing less than the fervent and unconditional dedication of our entire lives.

Dr. Sheldon Cooper - The Big Bang Theory

Agradecimentos

Inicialmente gostaria de agradecer ao Prof. Dr. Walter Filgueira de Azevedo Junior pela oportunidade e orientação ao longo desses anos. Por me permitir realizar meu treinamento científico no seu laboratório e, principalmente, pela confiança e liberdade que sempre me deu, permitindo assim a produção de uma série de trabalhos paralelos.

Minha gratidão ao Prof. Dr. Diógenes Santiago Santos e Prof. Dr. Luiz Augusto Basso, pois sem eles certamente não estaria cursando a minha Pós-Graduação na PUCRS e a eles devo a indicação para ser orientado pelo Prof. Dr. Walter F. de Azevedo Jr.

Ao meu amigo e meus dois braços direito Luis Fernando Saraiva Macedo Timmers, pela amizade, apoio e ajuda ao longo deste trabalho. Sem ele, certamente não só este trabalho, mas toda a produção durante este doutorado não seria possível.

Ao Guy Barros Barcelos agradeço pela amizade e apoio ao longo desses anos.

À Sabrina Moraes, pelo incentivo, apoio e carinho em todas as horas.

À minha mãe, Vera Maria Andrade, pelo amor incondicional, apoio em todas as horas difíceis. Fez dos meus sonhos os dela, e não mediu esforços para que pudesse realizá-los. Seria impossível transcrever o quanto sou grato a ela.

A todas as pessoas que direta ou indiretamente contribuíram para a execução deste trabalho.

Resumo

A tuberculose ressurgiu na metade dos anos 80 e, atualmente aproximadamente dois milhões de pessoas morrem por ano devido a esta doença. O ressurgimento da tuberculose tornou-se uma ameaça à saúde pública. A alta susceptibilidade dos pacientes infectados com HIV e a proliferação de cepas resistentes a múltiplas drogas têm criado a necessidade de se desenvolver novas terapias. No entanto, nenhuma nova classe de drogas contra a tuberculose foi desenvolvida nos últimos 45 anos. Deste modo, torna-se iminente a necessidade de se desenvolver novos agentes antituberculose.

Como o metabolismo de purinas pode estar implicado na latência da micobactéria, a purina nucleosídeo fosforilase de *Mycobacterium tuberculosis* (MtPNP) (EC 2.4.2.1) foi proposta como alvo para o desenvolvimento de drogas antibacterianas. A PNP catalisa a clivagem reversível, na presença de fosfato inorgânico, de ligações *N*-ribosídicas de nucleosídeos e desoxinucleosídeos de purina, com exceção da adenosina. Esta reação produz base púrica livre e ribose (desoxiribose)-1-fosfato. A reação se processa com inversão de configuração, de β-nucleosídeos para α-ribose-1-fosfato.

Neste trabalho a PNP foi cristalizada em associação com inosina, hipoxantina e aciclovir, substrato, produto e inibidor, respectivamente, e os dados foram coletados utilizando radiação síncrotron. Além disso, a simulação por dinâmica molecular e experimentos de calorimetria por titulação isotérmica foram utilizadas para fornecer informações detalhadas acerca das propriedades dinâmicas, e investigar o perfil termodinâmico e afinidades da MtPNP associada com estas moléculas. Com os resultados obtidos nós esperamos contribuir para a busca de novos inibidores seletivos de MtPNP, já que as diferenças entre os sítios de ligação da enzima humana e de micobactéria foram identificadas , tornando viáveis projetos de desenho de drogas baseados na estrutura.

Abstract

Tuberculosis re-emerged in the mid 80s and currently about two million people die each year due to this disease. The resurgence of tuberculosis has become a threat to public health. The high susceptibility of HIV-infected patients and the proliferation of multi-drug resistant strains have created the need to develop new therapies. However, no new class of drugs against tuberculosis was developed in the last 45 years. Thus, it becomes imminent need to develop new antituberculosis agents.

As purine metabolism could be implicated in mycobacterial latency the purine nucleoside phosphorylase (EC 2.4.2.1) has been proposed as target for development of antibacterial drugs. PNP catalyzes the reversible cleavage in the presence of inorganic phosphate of *N*-ribosidic bonds of the purine nucleosides and deoxynucleosides, except adenosine. This reaction generates the purine base and ribose (deoxyribose)-1-phosphate. PNP is specific for purine nucleosides in the β-configuration and cleaves the glycosidic bond with inversion of configuration to produce α–ribose-1-phosphate.

In this work PNP was crystallized in association with inosine, hypoxanthine and acyclovir, substrate, product and inhibitor, respectively, and data were collected using synchrotron radiation. In addition, molecular dynamics simulations and isothermal titration calorimetry experiments were used to provide detailed information on the dynamic properties and to investigate the profile and thermodynamic affinities of MtPNP associated with these molecules. With obtained results we hope to contribute to the search of new selective inhibitors for MtPNP, since differences between the mycobacterial and human enzyme binding sites have been also identified, making structure-based drug design feasible.

Lista de figuras

Lista de siglas e abreviaturas

ACY: Aciclovir

ADA: Adenosina deaminase

AIDS: Síndrome da imunodeficiência adquirida

BCG: Bacilo de Calmette-Guérin

BRICS: Grupos de países de economias emergentes constituídos de Brasil, Rússia, Índia, China e África do Sul.

CPBMF: Centro de Pesquisas em Biologia Molecular e Funcional

DM: Dinâmica molecular

DNA: Ácido desoxirribonucleico

HIV: Vírus da Imunodeficiência Humana

INO: Inosina

ITC: Calorimetria por titulação isotérmica

MTB: *Mycobacterium tuberculosis*

MtPNP: Purina nucleosídeo fosforilase de *Mycobacterium tuberculosis*

HsPNP: Purina nucleosídeo fosforilase de *Homo sapiens*

OMS: Organização Mundial da Saúde

PAS: Ácido p-aminosalisílico

PCA: Análise dos componentes principais

PDB: Protein Data Bank

PNP: Purina nucleosídeo fosforilase

PRPP: 5-fosfo-α-D-ribose 1-difosfato

R-1-P: Ribose-1-fosfato

TB: Tuberculose

Sumário

Capítulo 1

Introdução

1 Introdução

1.1 A tuberculose

As doenças infecciosas ainda são responsáveis pelo sofrimento e morte de centenas de milhões de pessoas e 90% das mortes causadas por esse tipo de enfermidade ocorrem em áreas tropicais e subtropicais, regiões nas quais estão presentes 80% de toda população mundial (Trouiller *et al.*, 2001). Entre estas doenças destacam-se a AIDS/HIV, infecções respiratórias, malária e tuberculose. A infecção pelo *Mycobacterium tuberculosis* (MTB)*,* também conhecido por bacilo de Koch foi identificado em 24 de março de 1882 por Robert Koch. O bacilo causador da tuberculose (TB) é a principal causa de mortes em humanos devido a um único agente infeccioso, podendo ser causada por outras bactérias do gênero *Mycobacterium,* como por exemplo, o *Mycobacterium africanum*, *M. microti* e *M. bovis.*

De acordo com a Organização Mundial da Saúde (OMS), um terço da população mundial está infectada com o MTB e a estimativa é que 10% desta fração desenvolva a doença ao longo de sua vida (WHO, 2004a; Bloom & Murray, 1992). Atualmente, mais de 9,4 milhões de pessoas desenvolvem a TB ativa (WHO, 2009), resultando na morte de 1,8 milhões de pessoas de acordo com a atualização do último relatório da OMS (WHO, 2009). A cada dia mais de 25 mil pessoas ficam doentes, sendo que cinco mil acabam morrendo (WHO, 2003). No Brasil, de acordo com o relatório da Fundação Nacional da Saúde (FUNASA), entre os anos de 1980 e 2004 a TB apresentou uma média de ocorrência de 85 casos/ano, resultando numa taxa de 5 a 6 mil mortes/ano, entretanto especialistas acreditam que o número

de óbitos possa chegar a 10 mil (Pivetta, 2004), já a OMS afirma no seu último relatório que são 8.400 mortes no país (WHO, 2009).

Apesar da TB ser considerada por muitos como uma doença do século XIX, na verdade ela nunca foi erradicada. Nos últimos anos tem-se verificado um aumento na sua incidência: apresentando, entre 1997 e 2000, um acréscimo de 1,8% de novos casos ao ano (Corbett *et al.* 2003). Estima-se que entre 2002 e 2020, caso não haja um esforço governamental guiado por políticas de saúde pública para controle da TB, mais de 150 milhões de pessoas ficarão acometidas deste mal, e a TB levará à morte mais de 38 milhões de pessoas (WHO, 2001; WHO, 2002). Dada a gravidade da situação global da doença, em 1993 a OMS declarou a TB um sério problema de saúde pública mundial, isto como forma de alertar os governos e seus setores de saúde pública para a necessidade de contenção desta doença. A TB é denominada a doença da pobreza, afetando principalmente adultos jovens, ou seja, na sua idade mais produtiva. Em sua vasta maioria, as mortes por TB ocorrem em países emergentes e mais da metade dos óbitos ocorrem no continente asiático.

A transmissão do bacilo ocorre por via aérea, devido à inalação de pequenas partículas de aerossóis expelidas através da fala, espirro e principalmente pela tosse dos infectados que possuem a forma pulmonar da doença. Estas partículas são inaladas pelo indivíduo sadio, atingido o espaço alveolar, onde inicia a multiplicação e são fagocitadas pelos macrófagos do hospedeiro (Hiriayanna & Ramakrishnan, 1986). Como o MTB é capaz de resistir ao ataque, sobreviver e multiplicar-se no interior das células fagocitárias, como os macrófagos, o bacilo é considerado um parasita intracelular (Clemmens, 1996). À medida que macrófagos, monócitos e células T são recrutados para a área em torno do bacilo, ele diminui sua replicação entrando no estado de latência até que haja um momento de deficiência do sistema

imunológico. O MTB normalmente sobrevive durante anos neste estado de dormência dentro dos tecidos (Manabe & Bishai, 2000).

A incidência de TB teve um rápido declínio no início do século XX em países em desenvolvimento, devido à melhora nas condições sanitárias e de moradias. Essa tendência foi acelerada inicialmente pela introdução da vacina BCG (Bacilo de Calmette-Guérin) em 1921 e da descoberta de antibióticos como a estreptomicina (1944), ácido ρ-aminosalisílico (PAS) em 1946, isoniazida (1952) e rifampicina (1965) (Drobniewski *et al.*, 2003; Duncan, 2003). Entretano dois principais fatores têm contribuído para o aumento no número de TB. O primeiro é a susceptibilidade de pacientes co-infectados com o vírus HIV, cujo sistema imunológico enfraquecido não consegue controlar o crescimento do bacilo. Estes pacientes apresentam um risco cem vezes maior de desenvolver a doença (El Sayed *et al.*, 2000). O segundo fator é o surgimento de cepas resistentes aos antimicrobianos de primeira linha (isoniazida e rifampicina) utilizados no tratamento, devido a terapias inadequadas, uso indiscriminado destes antibióticos (Baptista *et al*. 2002) e abandono do tratamento (Basso *et al*., 1998).

A prescrição mais comum para o tratamento da TB utiliza a combinação das drogas isoniazida, rifampicina, pirazinamida e etambutol (considerados agentes terapêuticos de 1ª linha) nos primeiros dois meses, com o intuito de exercer uma ação bactericida contra o bacilo ativo, e, posteriormente isoniazida e rifampicina para os últimos quatro meses de tratamento. A cicloserina, etionamida, o PAS, capreomicina e a estreptomicina são considerados fármacos de 2ª linha. A estreptomicina pertenceu durante muitos anos aos antibacilares de 1ª linha, atualmente devido ao aumento da resistência das cepas frente ao tratamento, sua utilização foi diminuída, sendo relegada para agentes de 2ª linha.

Os mecanismos de resistência aos agentes antituberculose são devido às alterações no DNA cromossomal, portanto estas cepas não estão sujeitas à seleção reversa, e permanecerão causando falha de tratamentos padrões contra TB. Devido a isso o desenvolvimento de novas drogas para substituírem aquelas comprometidas pela resistência é premente para o desenvolvimento de um tratamento quimioterápico eficaz. A pesquisa de novas drogas para TB ficou a cargo dos governos, já que laboratórios privados não demonstram interesse devido ao mercado não representar um atrativo do ponto de vista comercial como as demais drogas lançadas.

Como a incidência da TB ocorre principalmente em países de economia emergente, como o grupo econômico denominado BRICS (Brasil, Rússia, Índia, China e África do Sul), o mercado estimado para venda destes agentes antibacilares não compensaria o seu custo de pesquisa e desenvolvimento.

1.2 Metabolismo de nucleotídeos

Os nucleotídeos são moléculas de vital importância para todos os organismos. Eles são essenciais para a síntese de ácidos nucléicos, proteínas e outros metabólitos, assim como para reações que necessitam de energia. Em geral, os nucleotídeos de purinas podem ser sintetizados pela via *de novo*, que utiliza compostos simples para a síntese de vários nucleotídeos de purinas, e/ou pela via de salvamento, constituída por rotas de reutilização pelas quais as células podem satisfazer a necessidade de purinas a partir de fontes endógenas e/ou exógenas de purinas pré-formadas (el Kouni, 2003).

A síntese *de novo* inicia a partir de precursores simples, como aminoácidos, ribose-5-fosfato, CO_2 e NH_3, enquanto a via de salvamento está relacionada à reciclagem de bases livres e nucleosídeos formados no catabolismo de nucleotídeos.

As vias de síntese *de novo* e de salvamento de purinas e de pirimidinas são distintas nos seus mecanismos e em sua regulação, apresentando, no entanto, alguns precursores comuns, como o aminoácido glutamina como fonte de grupamentos amino, e PRPP (5-fosfo-α-D-ribose 1-difosfato) como fonte da porção pentose (Tozzi *et al*., 2010).

O metabolismo de purinas constitui um alvo potencial para o desenho racional de quimioterápicos antiparasitários e antibacilares. Isto se deve à algumas diferenças entre bactérias, parasitas e seus hospedeiros. Entre elas, a especificidade do transporte de purinas, podendo ter um alto grau de seletividade e também as diferenças relacionadas à preferência pelo substrato utilizado (Parker & Long, 2007; el Kouni, 2003). Embora qualquer uma das enzimas do metabolismo de purinas possa ser alvo para o desenvolvimento de drogas anti-TB, enzimas envolvidas no salvamento de purinas são de interesse particular. O objetivo do desenvolvimento de drogas desse tipo é identificar análogos de purinas que possam ser convertidos a nucleotídeos tóxicos em células do MTB, mas não em células humanas (Parker & Long, 2007).

1.3 Via de salvamento de purinas

A purina nucleosídeo fosforilase (PNP) é uma enzima que utiliza como substrato inosina (Ino) e guanosina para convertê-las em hipoxantina (Hx) e guanina

(Gua), respectivamente. A PNP catalisa a fosforólise da ligação glicosídica entre o átomo C1 da ribose e N9 da base nitrogenada. Assim, nucleosídeos são convertidos em bases livres, liberando ribose-1-fosfato (R-1-P) **(Figura 1)**.

Embora a adenosina não seja substrato da PNP em MTB, outra enzima, a adenosina deaminase (ADA) converte adenosina em Ino, que é convertida a Hx pela PNP. Em humanos, a Hx é catabolisada por outras enzimas a xantina e finalmente excretada pela urina como acido úrico. As bases livres geradas podem ser convertidas de volta a nucleotídeos pela ação de fosforibosiltransferases específicas da via de salvamento, ou degradadas.

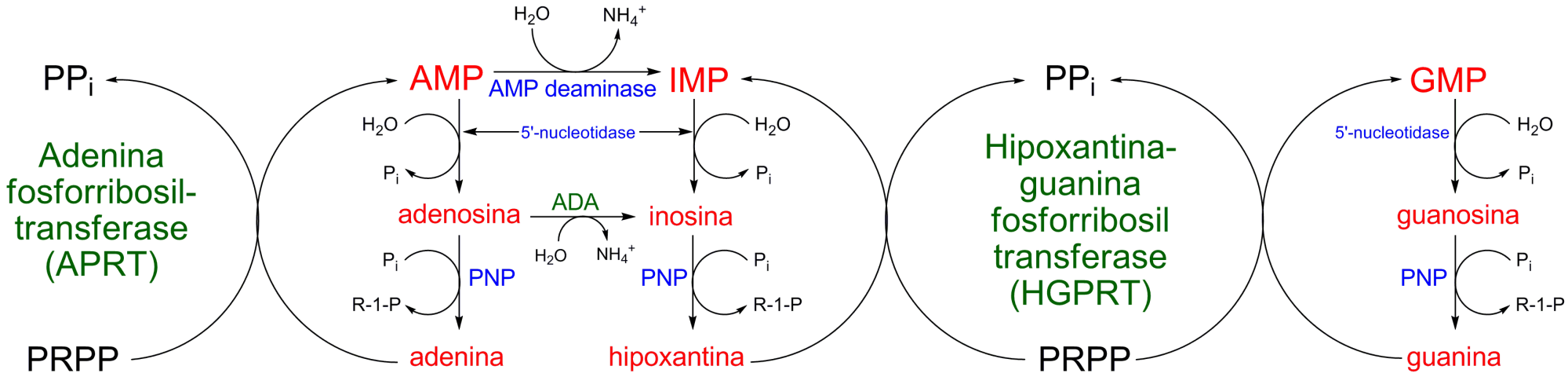

Figura 1 - Via de salvamento de purinas.

As reações catalisadas pelas enzimas da via de salvamento de purinas são reversíveis e atuam também no catabolismo destes nucleotídeos, sendo o sentido das reações (salvamento ou catabolismo) determinado pelas condições da célula.

No catabolismo, a base livre hipoxantina gerada pela clivagem do IMP é convertida em xantina pela xantina oxidase, e guanina é deaminada pela ação da guanase a xantina. A xantina é convertida em acido úrico pela xantina oxidase, que é excretado na urina. Pouca energia é obtida da degradação de purinas, o que torna a via de salvamento energeticamente mais favorável para a célula.

Com relação ao MTB há muito pouca informação específica sobre o metabolismo de purinas, entretanto, é conhecido que o bacilo expressa todas as enzimas necessárias para a síntese *de novo* dos nucleotídeos de purina e, seu metabolismo, é similar ao que ocorre em células humanas e outros organismos. No entanto, podem ocorrer variações importantes e uma regulação diferenciada da expressão e da atividade das enzimas que compõem o metabolismo de purinas no gênero de *Mycobacterium*. No sequenciamento do genoma de MTB foram identificados genes que são capazes de expressar ADA e PNP. Esta última possui uma sequência e estrutura similar a PNP humana e não reconhece adenosina como substrato, divergindo de outros organismos.

1.4 Purina nucleosídeo fosforilase de *Mycobacterium tuberculosis*

A PNP tem um papel central no metabolismo de purinas, operando normalmente na via de recuperação nas células (De Azevedo *et al.*, 2003). A PNP catalisa a clivagem da ligação N-glicosídica de ribo e desoxirribonucleosídeos, na presença de ortofosfato inorgânico (Pi) como um segundo substrato, para gerar uma base púrica livre e a (desoxi/ribose)-1-fosfato **(Figura 2)** (Canduri *et al.*, 2004).

Independentemente da origem celular as PNPs estão subdivididas de acordo com a sua estrutura quaternária, sendo elas: homotriméricas (baixo peso molecular, PNP-I) e homohexaméricas (alto peso molecular, PNP-II). As PNPs homotriméricas são altamente específicas para 6-oxopurinas, seus nucleosídeos e alguns análogos; considerando que PNPs homohexaméricas adicionalmente aceitam 6-aminopurinas, seus nucleosídeos, e outros análogos (Bzowska *et al.*, 2000).

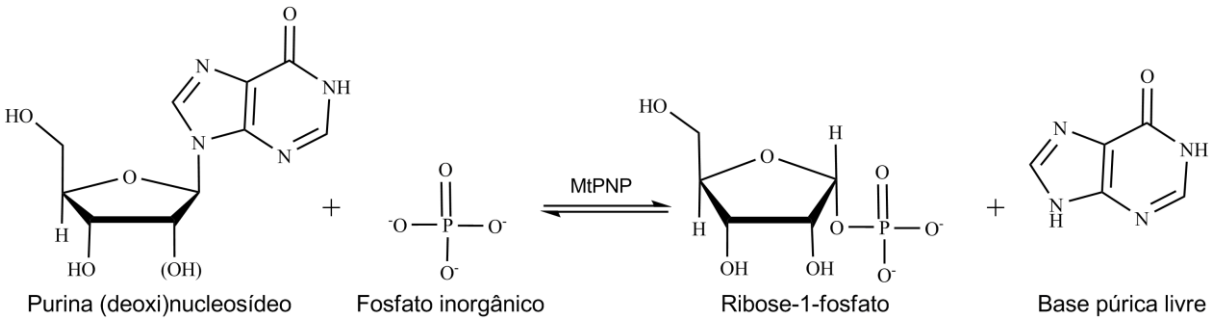

Figura 2 - Reação catalisada pela MtPNP. Nota-se que a inserção do fosfato na pentose ocorre concomitantemente com a inversão de sua ligação.

A PNP de MTB (MtPNP) é codificada pelo gene *deoD* (Rv3307, 807 pb, 268 aminoácidos, 27.539,4 Da, e pI = 5.75), alternativamente chamado *punA*, é um membro da classe homotrimérica (Basso *et al.*, 2001). Esta classe inclui a PNP humana (HsPNP) e homólogos bovinos, entre outros. As PNPs pertencentes à classe trimérica diferem significativamente da classe hexamérica, que usualmente estão presente em procariotos (Bzowska *et al.*, 2000; Jensen & Nygaard, 1975). O

homólogo na micobactéria é mais específica ao nucleosídeo natural 6-oxopurina (Ino, desoxiinosina, guanosina e 2-desoxiguanosina (2dGuo)) e compostos sintéticos, que não catalisa a fosforólise de adenosina (Ducati *et al.*, 2009). Esta especificidade pelo substrato esta de acordo com o conceito de que as PNPs não podem catalisar a fosforólise e/ou a síntese de nucleosídeos de 6-aminopurinas de forma apreciável (Zimmerman *et al.*, 1971; Stoeckler *et al.*, 1997).

Surpreendentemente, a MtPNP parece desempenhar um papel fundamental na sobrevivência do bacilo, uma vez que uma cepa com o respectivo gene silenciado não é viável, devido à essencialidade inesperada do gene (resultados não publicados). Este resultado ressalta a necessidade de demonstrar a função da proteína por abordagens computacionais e experimentais em vez de atribuir a função a um gene específico com base apenas em dados comparativos.

A MtPNP é constituída predominantemente por resíduos de alanina (17.5%), leucina (12.3%), valina (10.1%), e glicina (10.4%). Como previamente mencionado, PNPs com diferentes especificidades tem sido identificadas, e, em vários casos, purificadas a partir de uma ampla gama de organismos. Considerando que a maioria das PNPs derivadas de bactérias são hexaméricas, a MtPNP torna-se uma exceção à regra revelando ser um homotrímero simétrico com um arranjo triangular de subunidades semelhantes às estruturas de PNP de mamíferos (Shi *et al.*, 2001) **(Figura 3)**.

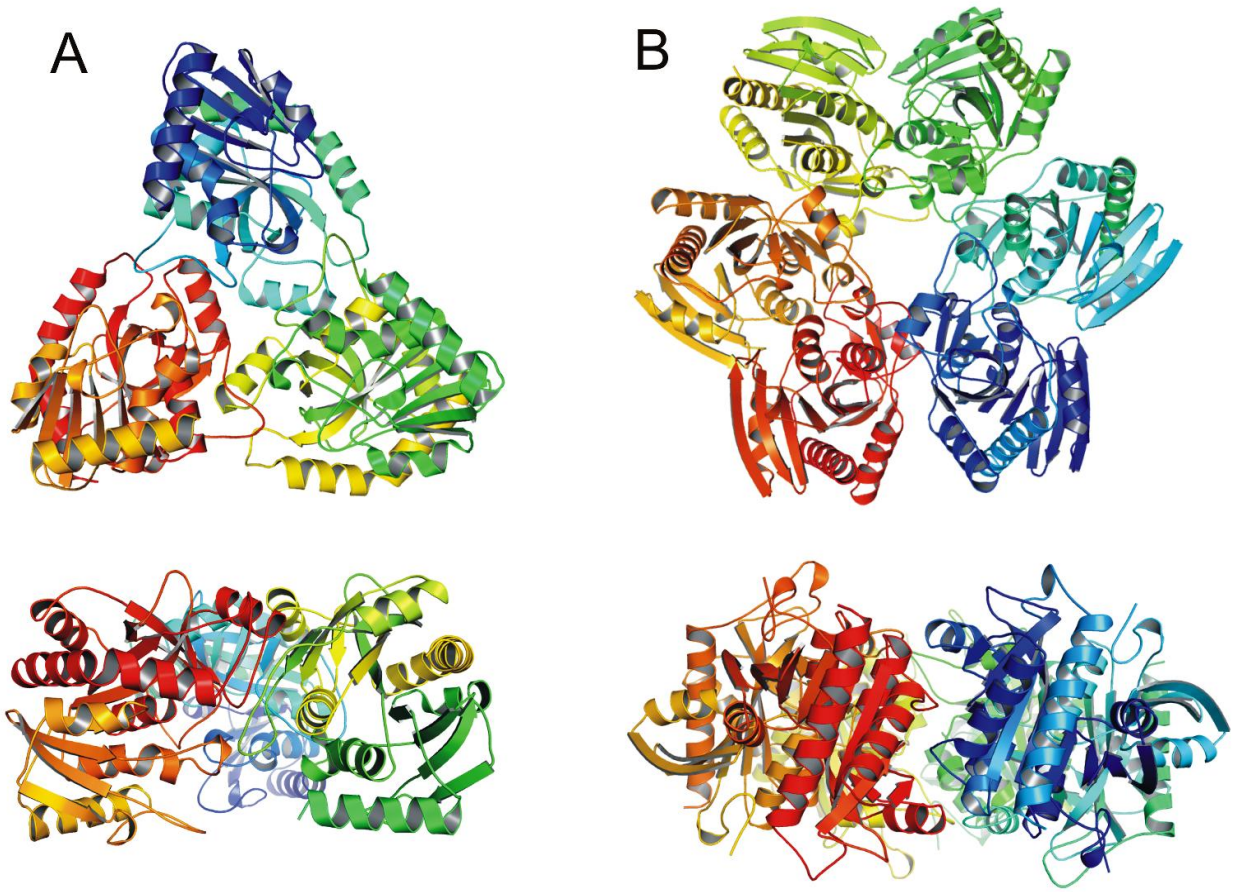

Figura 3 - Estrutura de PNP (A) trimérica (PDB: 1G2O (Shi *et al.*, 2001)) e (B) hexamérica PNP (PDB: 1NW4 (Shi *et al.*, 2004)).

Em 2001, Shi e colaboradores (Shi *et al.*, 2001) resolveram, pela primeira vez, as estruturas da MtPNP complexada com Imucilina-H (ImmH) e fosfato (PO_4), e com Iminoribitol, 9-deazahipoxantina, e PO_4. As estruturas cristalográficas foram depositadas no *Protein Data Bank* (PDB (Berman *et al.*, 2002)) sob os códigos 1G20 e 1I80 (Shi *et al.*, 2001). Estas estruturas forneceram uma imagem detalhada da conformação catalítica da MtPNP quando ligada à um análogo do substrato em seu estado de transição.

Cada monômero da proteína está enovelado num único domínio (α/β) contendo nove fitas β e nove hélices α **(Figura 4)**. O núcleo consiste de uma folha β (β2, Thr50-Gln54; β3, Gly70-Ile77; β4, His80-Glu87; β1, Val30-Leu34; β5, Gln113-

Leu124; β9, Gln222-Thr230; β6, Gln132-Leu142; e β7, Ala176-Leu183) cercado por nove hélices α (α1, Pro8-Thr23; α2, Val42-Ala44; α3, Arg98-Tyr99; α4, Pro103-Ser110; α5, Pro162-Ser171; α6, Pro191-Leu200; α7, Val210-Ala219; α8, His243-Ala251; e α9, Thr255-Arg267). Sendo que, β5 e β9 são estendidas e participam de um pequeno barril β distorcido (β9; β5; β8; Asp203-Gly206; β7; e β6). É importante ressaltar que todas as estruturas secundárias descritas aqui foram identificadas utilizando o software Swiss-PdbViewer v.4.0 (Guex & Peitsch, 1997). Estes elementos estruturais secundários estão conectados por alças estendidas, uma característica comum a todas as estruturas de PNPs resolvidas até o momento.

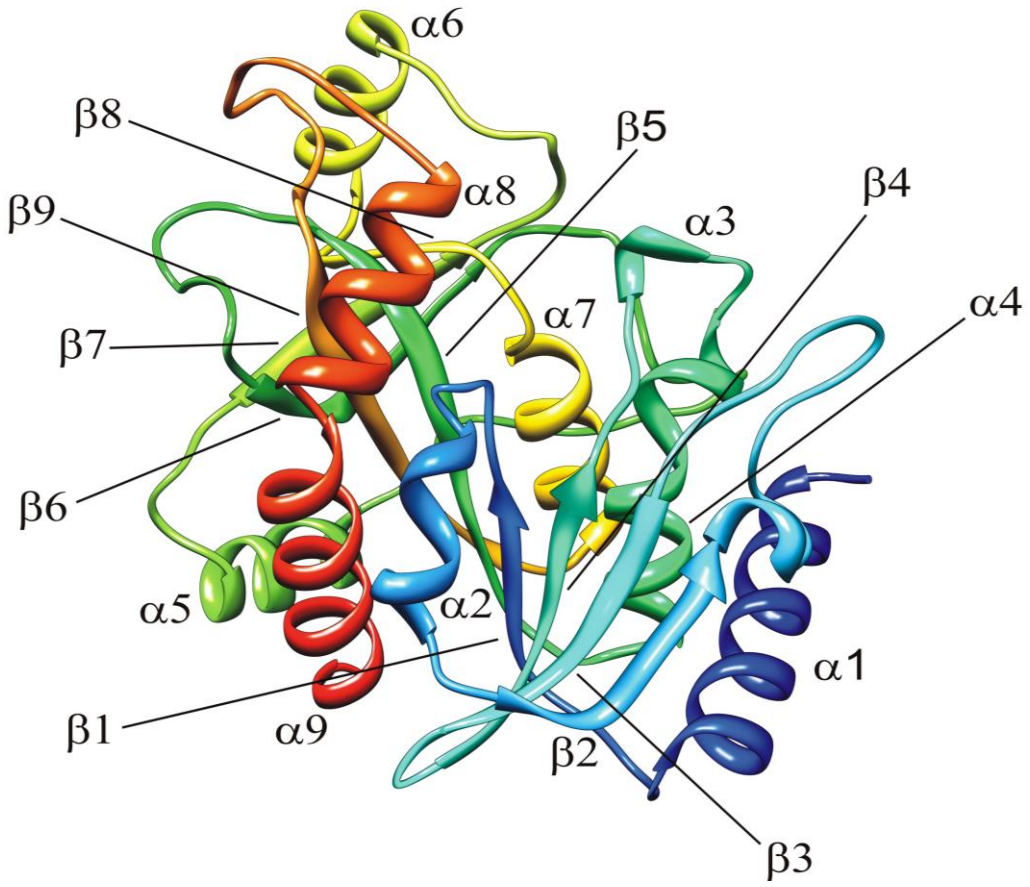

Figura 4 - Estrutura secundária do monômero da MtPNP (PDB: 3IOM (Ducati *et al.*, 2010)).

No entanto, se comparado com outras (PDB:3IOM (Ducati *et al.*, 2010), PDB:1I80 (Shi *et al.*, 2001), e MtPNP:Hx (a ser publicado)), esta alça apresenta um alto desvio médio quadrático (RMSD) de 8,2 Å, 8,4 Å, e 8,2 Å, respectivamente. Os resíduos desta alça não interagem diretamente com o inibidor ligado ou o PO_4, mas estão envolvidas na orientação das cadeias laterais dos resíduos dos sítios ativos (Shi *et al.*, 2001).

Contatos entre cada subunidade envolvem resíduos do Alça4 (Ala65), Alça5 (Tyr92-Glu93), β6 (Asp138-Leu142), Alça7 (Thr143-Ala159), β7 (Val179), Alça8-α6 (Pro184-Leu200), Volta (Met207), α7 (Ile214), e Alça9-α8 (Ala234-His243). As sete interações, por meio de ligação de hidrogênio nas interfaces da subunidade incluem Tyr92(A) O-N Gly150(B), His187(A) ND1-OG Ser146(B), Tyr188(A) N-O Val154(B), Leu241(A) N-OD1 Asp155(B), Ala192(A) N-OD2 Asp138(B), Thr190(A) OG-O His139(B), e Glu193(A) OE2-N Asn141(B). Interações hidrofóbicas de van der Waals envolvendo os pares de resíduos Tyr92(A)-Phe153(B), Tyr188(A)-Phe153(B), His243(A)-Phe153(B), His187(A)-Ile214(B), His187(A)-Leu156(B), Thr190(A)-Asp138(B), Thr190(A)-His139(B), Ala192(A)-Asp138(B), Glu193(A)-Leu140(B), e Met196(A)-Leu142(B).

Nas PNPs triméricas, todo o sítio ativo está localizado mais internamente na estrutura da proteína, que pode ser dividida em três partes: o sitio de ligação de fosfato, o qual, em algumas estruturas, ocupado pelo sulfato (utilizado em altas concentrações em condições de cristalização), o sítio de ligação de pentose e o da base **(Figura 5)**. O sítio ativo de cada monômero está localizado na interface dos dímeros e a distância entre os sítios ativos de cada monômero é de aproximadamente 30,0 Å.

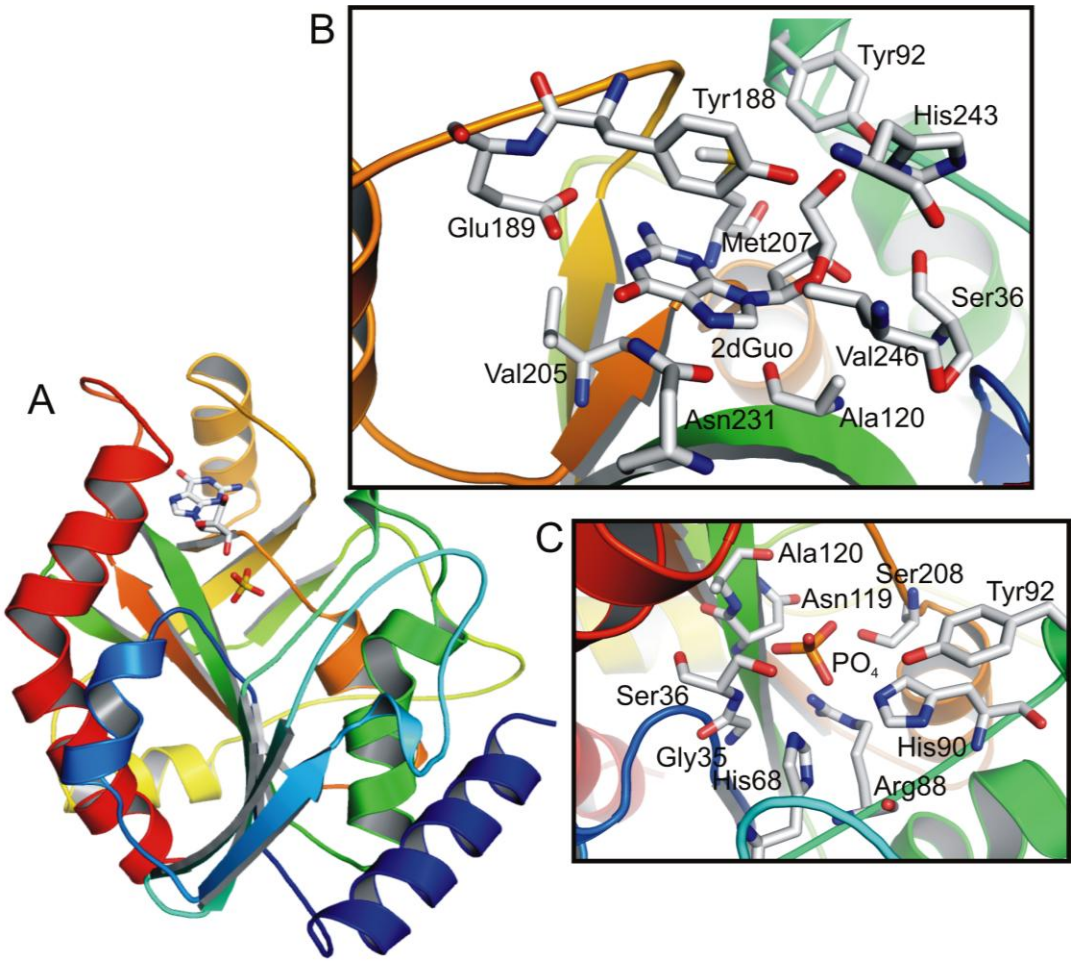

Figura 5 - Sítios de ligação da MtPNP. (A) Monômero da MtPNP (PDB: 3IOM (Ducati *et al.*, 2010)) complexado com sulfato e 2dGuo. (B) Sítio de ligação de pentose e base (PDB: 3IOM (Ducati *et al.*, 2010)). (C) Sítio de ligação de fosfato (PDB: 1G2O (Shi *et al.*, 2001)).

1.5 Desenho de drogas baseado em estrutura

A cristalografia de proteínas é uma ferramenta essencial para a descoberta e investigação de interações farmacológicas a nível molecular. A estrutura cristalográfica da MtPNP fornece valiosas informações para o desenho de drogas antimicobacterianas baseadas na estrutura, uma vez que ela captura os detalhes de um sítio ativo. No entanto, foi demonstrado que os sítios de ligação de pentose e da base podem acomodar moléculas que diferem dos seus substratos naturais, por isso muito cuidado deve ser mantido quando simulações de docagem molecular são realizadas no intuito de se encontrar inibidores seletivos para MtPNP (Ducati *et al.*, 2010). O desenvolvimento de novos inibidores seletivos para MtPNP ainda é um desafio, pois eles apresentam elevada toxicidade, tornando-os impróprios para administração a seres humanos. Assim, os esforços para o desenvolvimento de novas drogas com toxicidade seletiva baseada em diferenças estruturais entre MtPNP e HsPNP devem ser buscadas.

Capítulo 2

Justificativa

2 Justificativa

Os dados referente à TB fornecido pela OMS, tanto incidência, número de novos casos e principalmente a emergência de cepas resistentes aos quimioterápicos, por si só justificam a necessidade à busca de novos alvos moleculares e principalmente novas drogas. É urgente a necessidade de novos agentes quimioterápicos para o tratamento da TB, os quais visem diminuir a toxicidade e a duração do tratamento atual. O tempo de tratamento é um dos problemas cruciais para o surgimento de cepas resistentes, como a MDR-TB (multirresistente), XDR-TB (extensivamente multirresistente) e TDR-TB (totalmente resistentes (Velayati *et al*., 2009)), às drogas comercialmente disponíveis. Outro agravante para o tratamento ocorre devido ao fato de que os fármacos utilizados para TB e HIV compartilham rotas metabólicas, o que diminui a sua eficiência e intensifica os efeitos colaterais sobre os pacientes.

Não há a necessidade de uma formação epidemiológica para concluirmos que a TB é uma tragédia global anunciada. No caso do Brasil, a epidemia de *crack* que grassa o país agrava a situação do tratamento dos infectados, já que os dependentes apresentam uma menor aderência ao tratamento fornecido pelos municípios através Sistema Único de Saúde.

Tendo em vista estas considerações, uma melhor compreensão estrutural da MtPNP e sua interação com seus substratos, através da cristalografia de proteínas e simulação por dinâmica molecular permitirá o delineamento de novas estratégias no que se refere o desenvolvimento de inibidores mais seletivos, pois há indícios que esta enzima pode ter um papel importante no estado de latência do bacilo.

Capítulo 3

Objetivos

3.1 Objetivo geral
3.2 Objetivos específicos

3 Objetivos

3.1 Objetivo geral

Este projeto de pesquisa pretende realizar estudos estruturais de PNP de *Mycobacterium tuberculosis* utilizando cristalografia de raios X, bioinformática estrutural e biofísica computacional, através do método de Dinâmica Molecular (DM). A utilização do método de DM tem o intuito de avaliar o comportamento dinâmico da MtPNP em solução.

3.2 Objetivos específicos

- Obtenção de cristais de MtPNP complexada com o substrato Ino e seu produto Hx, já que somente o complexo MtPNP:2dGuo que foi resolvido recentemente apresenta um dos substratos; E obtenção do complexo MtPNP com aciclovir (ACY);
- Determinar a estrutura tridimensional destas proteínas, a partir da técnica de biocristalografia;
- Simular os complexos de MtPNP obtidos através da técnica de DM para melhor compreender a influência dos substratos sobre o sítio catalítico em solução;
- Identificar aspectos estruturais determinantes para a seletividade das respectivas moléculas pela MtPNP.

Capítulo 4

Metodologia

4.1 A proteína
4.2 Cristalografia de macromoléculas biológicas
4.3 Técnica de cristalização de macromoléculas biológicas
4.4 Dinâmica molecular
4.5 Análise dos componentes principais

4 Metodologia

4.1 A proteína

A proteína MtPNP utilizada neste projeto, foi produzida e purificada no Centro de Pesquisas de Biologia Molecular e Funcional (CPBMF-TecnoPUC), laboratório coordenado pelos Prof. Dr. Diógenes Santiago Santos (PUCRS) e Prof. Dr. Luiz Augusto Basso (PUCRS).

4.2 Cristalização de macromoléculas biológicas

A determinação e análise das estruturas tridimensionais por difração de raios X tem por objetivo essencial o conhecimento da estrutura molecular e cristalina dos materiais. Através desta metodologia podem-se determinar as posições relativas de todos os átomos que constituem a molécula (estrutura molecular) e a posição relativa de todas as moléculas que constituem a cela unitária (estrutura cristalina).

O uso desta técnica, juntamente com estudos bioquímicos, tem auxiliado na investigação das bases moleculares das atividades biológicas das proteínas de interesse (Blundell & Johnson, 1976).

Para se determinar a estrutura tridimensional de uma macromolécula por técnicas de difração de raios X é essencial a obtenção de monocristais de tamanho apropriado para a coleta de dados de difração de raios X. Como o número de variáveis envolvidas no processo de cristalização é muito grande (como concentração de sal, temperatura, pH, agentes precipitantes e aditivos) encontrar as

condições ideais pode levar dias, meses, anos ou pode ainda nunca acontecer (Blundell & Johnson, 1976).

Para cristalizar uma macromolécula em um determinado solvente é necessário leva-la lentamente a um estado de supersaturação, que é termodinamicamente instável, na qual pode-se chegar a uma fase amorfa (precipitação) ou cristalina.

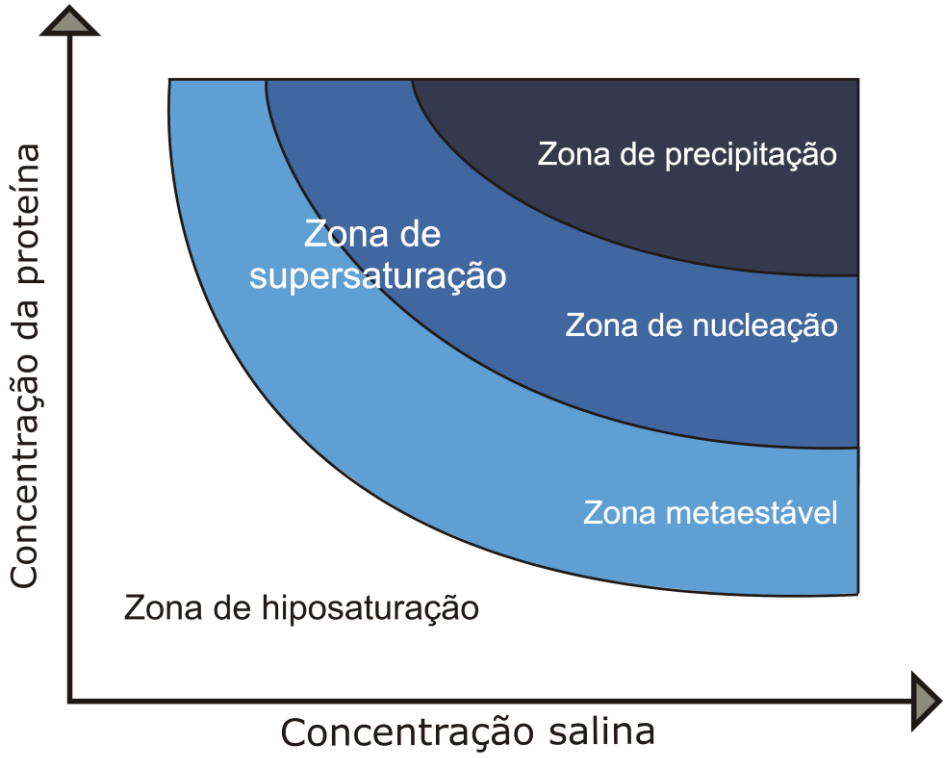

Figura 6 - Representação esquemática de um diagrama de solubilidade.

A cristalização é um processo de ordenação no qual as moléculas assumem posições regulares no estado sólido. Um processo de cristalização pode ser considerado como um equilíbrio dinâmico entre as partículas no estado líquido e no estado sólido. Sendo assim, o cristal cresce quando o equilíbrio é deslocado no sentido de solidificação. A curva de solubilidade (**Figura 6**) divide as regiões de hiposaturação e de supersaturação. Na região de hiposaturação a macromolécula

não será cristalizada, ela estará completamente solúvel. Logo acima se encontra a região de supersaturação, que é dividida em três zonas: zona metaestável, zona de nucleação e zona de precipitação. Quando a supersaturação é alcançada rapidamente, a proteína em solução precipita. No entanto, quando a supersaturação é alcançada lentamente, a solução de proteína alcança a zona de nucleação, onde se formam os núcleos (primeiros agregados ordenados de proteína). Conforme a solubilidade da proteína diminui, os núcleos atingem a zona metaestável, onde ocorrerá o crescimento do cristal (Ducruix & Giegé, 1992). Na zona metaestável não há nucleação nem formação de agregados cristalinos, nesta região somente há manutenção ou crescimento dos cristais. O gerenciamento das concentrações da proteína e da solução salina, conhecida também com solução do poço, permite o controle da formação e crescimento dos cristais.

4.3 Técnica de cristalização de macromoléculas biológicas

Existem muitas técnicas de cristalização de macromoléculas biológicas, porém todas têm um único objetivo, trazer a solução da macromolécula a um estado de supersaturação. Basicamente são utilizadas quatro técnicas para a cristalização de macromoléculas biológicas: diálise, difusão em interface livre, *batch* e difusão de vapor. Sendo a difusão de vapor um método bastante eficiente para o aumento gradativo da concentração do agente precipitante.

O princípio deste método é o processo de equilíbrio de duas soluções onde uma é formada por agente precipitante com alta concentração, e a outra pelo mesmo agente precipitante somado a proteína. Em meio hermeticamente fechado, a solução menos concentrada perderá seu solvente mais volátil até que o potencial químico de ambas as soluções se igualem. Um cristal tende a se formar à medida que a concentração do precipitante e, consequentemente, da proteína aumente gradativamente (Ducruix & Giegé, 1992). Para o método de difusão de vapor podem ser utilizados os sistemas: *hanging drop* (“gota suspensa”), *sitting drop* (“gota sentada”) e *sandwich drop* (“gota sanduíche”). O sistema *hanging drop* (**Figura 7**) é um dos métodos mais utilizados e adequados para testes iniciais com um grande número de condições de cristalização, já que utilizam pequenos volumes de solução da proteína (0,5 - 5,0 µL) além de facilitar a análise dos experimentos. Neste sistema a solução proteica somada à solução precipitante forma a gota suspensa e a solução precipitante (mais concentrada) é adicionada no reservatório.

A concentração da gota contendo solução de proteína mais solução de precipitante será equilibrada contra a solução precipitante do reservatório que, geralmente, está 50% mais concentrada em relação à gota, pois para a preparação da gota, adiciona-se uma alíquota de proteína à mesma quantidade de solução

precipitante contida no poço. O equilíbrio prossegue por meio da difusão de vapor de substâncias voláteis (água e/ou solventes orgânicos) até que a pressão de vapor da gota se iguale a solução do reservatório. Se o equilíbrio ocorrer por meio de troca de vapor da gota para o reservatório, haverá uma diminuição do volume da gota e, consequentemente, um aumento na concentração de todos os constituintes da gota.

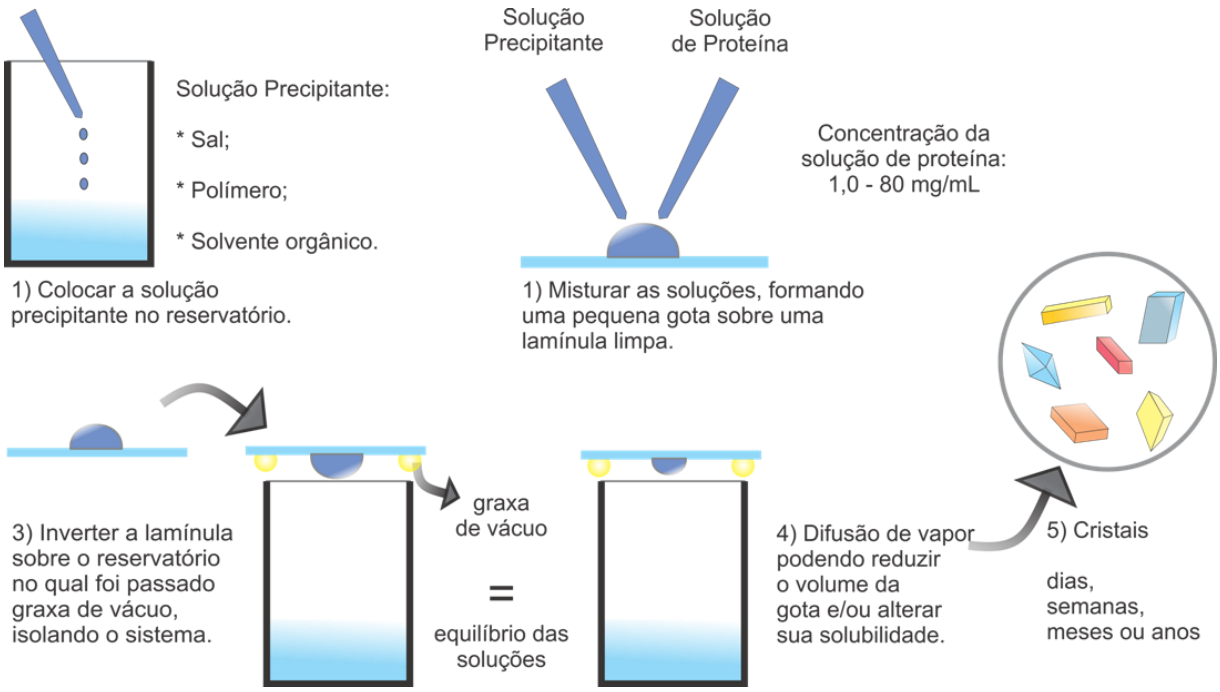

Figura 7 - Representação esquemática da sequência de eventos para a montagem do método de cristalização por difusão de vapor por gota suspensa.

4.4 Dinâmica molecular

Apesar de extremamente poderosa a técnica de cristalografia de macromoléculas biológicas ela possui uma grande limitação, ela não permite uma maior investigação acerca dos movimentos dos domínios ou resíduos que compõe a macromolécula. O modelo cristalográfico é apresentado como uma estrutura rígida e única, e processos biológicos envolvem, na sua maioria, mudanças conformacionais. Neste contexto as simulações por dinâmica molecular (DM) têm sido amplamente utilizadas para investigação da estrutura, função de biomoléculas e seus respectivos complexos e suas interações no processo de planejamento de fármacos assistido por computador. Esta técnica incorpora flexibilidade do ligante e receptor, melhorando suas interações e reforçando a complementaridade entre eles. Além disso, a capacidade de incorporar moléculas de solvente nas simulações dos sistemas receptor-ligante é muito importante para o entendimento do papel da água e seus efeitos sobre a estabilidade dos complexos proteína-ligante.

A simulação de DM consiste da solução numérica, passo a passo, da equação de movimento, que pode ser descrita para um sistema atômico simples pela equação abaixo (Equação 1)(van Gunsteren & Berendsen, 1990):

$$F_i(t) = m_i a_i \qquad \text{Equação 1}$$

onde F_i é a força que atua sobre cada partícula do sistema em um instante de tempo t, e a_i é a aceleração do átomo i de massa m_i.

Uma vez definido o campo de força, é possível calcular as forças que atuam sobre cada átomo, calculando-se a derivada primeira da energia potencial, obtida do

campo de força escolhido, em relação às posições desses átomos (equação 2) (van Gunsteren & Berendsen, 1990).

$$F_i(t) = -\frac{\partial V(r_i)}{\partial r_i}$$ Equação 2

Assim, as equações do movimento de Newton representam um sistema de *N* equações diferenciais acopladas (Marion & Thornton, 1995):

$$F_i = \frac{d}{dt} p_i = m_i \frac{d}{dt} v_i = m_i \frac{d^2}{dt} r_i$$ Equação 3

Sendo p_i o *momentum* do átomo *i*, de massa m_i com velocidade v_i e posição r_i . As soluções podem ser obtidas através da escolha adequada de coordenadas e velocidades iniciais para os *N* átomos.

Em simulações por DM, as soluções da equação 3 são obtidas numericamente por um Algoritmo Integrador. O Algoritmo Integrador realiza a integração das equações de movimento baseado nos métodos das diferenças finitas, nos quais a integração é dividida em pequenos intervalos de tempo (passos de integração) *Δt*, permitindo simular os movimentos de maior frequência do sistema, que muitas vezes são as vibrações das ligações (Verlet, 1968). Um dos métodos mais utilizados em dinâmica molecular para integrar as equações de movimento é o algoritmo de Verlet (Verlet, 1968; Allen & Tildesley, 1987), que utiliza as posições e acelerações dos átomos no tempo *t* e as posições do passo anterior, *r (t-Δt)*, para determinar as novas posições no tempo *t+Δt*, de acordo com a Equação 4 (van Gunsteren & Berendsen, 1990):

$$r(t+\Delta t) = 2r(t) - r(t-\Delta t) + a(t)\Delta t^2$$ Equação 4

4.5 Análise dos componentes principais

A função da proteína está relacionada com a sua estrutura e um dos principais objetivos da simulação de proteínas é gerar configurações suficientes do sistema de interesse para extrair movimentos e conformações funcionalmente relevantes. Uma dessas ferramentas para reduzir a dimensionalidade da trajetória gerada por DM para um subespaço essencial englobando alguns graus de liberdade, eliminando as flutuações de posicionamento, é a análise de componentes principais (PCA) (Hayward *et al.*, 1994; Mascarenhas *et al.*, 2010). PCA é um método comumente usado para dissecar a dinâmica de proteínas e sua importância nos processos biológicos, como o enovelamento de proteínas ou interação de substrato com a sua respectiva enzima. A análise PCA é uma técnica que reduz a complexidade dos dados e extrai o movimento concertado em simulações que são essencialmente correlacionadas e presumivelmente, significativas para função biológica (Amadei *et al.*, 1993). Na análise de PCA, a matriz de variância/covariância é construída a partir da trajetória após a remoção dos movimentos de rotação e translação. Um conjunto de autovetores e autovalores são identificados através de uma matriz diagonalizada. Os autovalores representam a amplitude dos autovetores ao longo do espaço multidimensional **(Figura 8)**, e os deslocamentos de átomos ao longo de cada autovetor apresentam as propostas concertadas da proteína ao longo de cada direção. Um pressuposto da análise de PCA é que os movimentos relacionados para a função da proteína são descritos por autovetores com autovalores numericamente significativos. Os movimentos essenciais da proteína no

subespaço são identificados através da projeção da trajetória de coordenadas cartesianas ao longo dos autovetores mais importantes da análise.

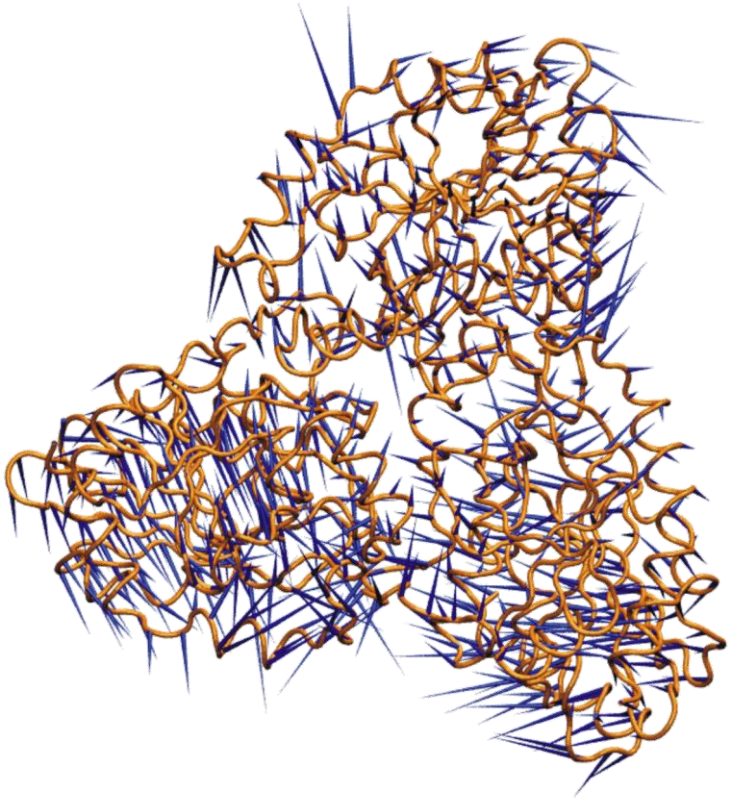

Figura 8 – Representação *porcupine* da simulação por DM de 20ns da MtPNP complexada com Hx (PDB: 3SCZ). O tamanho dos espinhos indica a amplitude (*eigenvalues*) e a direção (*eigenvectors*) do movimento ao longo da DM.

Esta metodologia permite uma diminuição da quantidade e da complexidade de dados gerados pela DM, o que em termos práticos significa uma melhor análise das conformações preponderantes numa dada simulação.

Capítulo 5

Purine Nucleoside Phosphorylase as a Molecular Target to Develop Active Compounds Against *Mycobacterium tuberculosis*

Revisão publicada no International Review of Biophysical Chemistry

Purine Nucleoside Phosphorylase as a Molecular Target to Develop Active Compounds Against *Mycobacterium tuberculosis*

Rodrigo G. Ducati[1], André A. Souto[1], Rafael A. Caceres[2], Walter F. de Azevedo Jr.[2], Luiz A. Basso[1,*], Diógenes S. Santos[1,*]

Abstract – *Despite the availability of chemotherapic and prophylactic approaches to fight consumption, human tuberculosis (TB) continues to claim millions of lives annually, mostly in developing nations, generally due to limited resources available to ensure proper treatment and where human immunodeficiency virus infections are common. Moreover, rising drug-resistant cases have worsened even further this picture. Accordingly, new therapeutic approaches have become necessary. The use of defined molecular targets could be explored as an attempt to develop new and selective chemical compounds to be employed in the treatment of TB. The present review highlights purine nucleoside phosphorylase, a component enzyme of the purine salvage pathway, as an attractive target for the development of new antimycobacterial agents, since this enzyme has been numbered among targets for Mycobacterium tuberculosis persistence in the human host. Enzyme kinetics and structural data are discussed to provide a basis to guide the rational anti-TB drug design.*

Keywords: *Enzyme Kinetics and Structural Analysis, Human Tuberculosis, Mycobacterium tuberculosis, Purine Nucleoside Phosphorylase, Rational Drug Development*

I. INTRODUCTION

Human tuberculosis (TB), mainly due to *Mycobacterium tuberculosis* infection, remains a leading cause of mortality due to a single infectious agent. This aerobic pathogenic bacterium usually establishes its infection in the lungs, and its progression is fundamentally regulated by the integrity of the host's immune system. This disease is mostly distributed among developing nations, generally due to limited resources available to ensure proper treatment and where human immunodeficiency virus infections are common.

From a historic point of view, the introduction of effective chemotherapic and prophylactic measures against TB have drastically reduced human deaths worldwide. However, history has also given us clear evidence that this is no longer true. This versatile infectious agent has evolved to adapt to the conditions imposed by the human host to survive. The resumption of consumption has been basically attributed to the recent generation of drug-resistant strains, capable of overcoming the chemical action of the currently administered agents, and thereby, being associated to greater morbidity and mortality [1].

Clearly, new approaches to combat TB have become needed. The use of defined molecular targets could be explored as an attempt to develop new and selective chemical compounds to be employed in the treatment of this disease. Particular features of this pathogen, such as enzymes from fundamental metabolic pathways with unique characteristics when compared to the human host could be evaluated to direct efforts towards target-based drug development [2]–[5].

The present review is focused on *M. tuberculosis* purine nucleoside phosphorylase (PNP; EC 2.4.2.1), a component enzyme of purine salvage pathway [3]. *M. tuberculosis* PNP is an attractive target for the development of new antimycobacterial agents, as it has been numbered among targets for *M. tuberculosis* persistence in humans (www.webtb.org). Enzyme kinetics and structural data have been included to provide a thorough knowledge on which to base the search for compounds with biological activity.

II. SELECTIVE DRUG DEVELOPMENT

II.1. Defining a molecular target

The complete genome sequencing of *M. tuberculosis* H37Rv strain [6] has made a decisive contribution to the field of research on TB, offering the scientific community a databank on which to explore singular features of this pathogen, thereby establishing a new phase in the battle against this pathogen. This particular strain has had a great

Manuscript received and revised xx 2010, accepted xx 2010

application in biomedical research worldwide due to total virulence retention in animal models, besides being susceptible to drugs and amenable to genetic manipulation [6].

The identification and validation of microbial essential pathways are important as a first step towards specific inhibitor design with low toxicity [7], since their component enzymes can be evaluated as possible targets for drug development. Homologues to enzymes of the purine salvage pathway have been identified in the genome sequence of *M. tuberculosis* H37Rv [6]. This pathway represents an essential cellular process that is critical for many organisms [8]. Since purine metabolism has been implicated in mycobacterial latency [9][10], it may offer a great opportunity to gather knowledge on a defined molecular target on which to base rational drug development efforts.

II.2. The candidate

PNP, a component enzyme of the purine salvage pathway [3], plays a critical role in the reversible phosphorolysis of the *N*-glycosidic bond of β-purine (deoxy)ribonucleosides to generate α-(deoxy)ribose 1-phosphate (R1P) and the corresponding purine bases [8][11]. Irrespective of the cellular origin, PNPs have been structurally subdivided according to their quaternary structures into the homotrimeric (low molecular weight; PNP-I) and homohexameric (high molecular weight; PNP-II) classes. Substrate specificities are considerably dissimilar among these classes, as a consequence of the substantial divergence of residue composition at the catalytic site [12][13]. Homotrimeric PNPs are highly specific for 6-oxopurines, their nucleosides, and some analogues; whereas homohexameric PNPs additionally accept 6-aminopurines, their nucleosides, and many analogues [13].

The enzyme from *M. tuberculosis* (MtPNP), encoded by the *deoD* gene (Rv3307, 807 bp, 268 aa, 27539.4 Da, and pI = 5.75), alternatively named *punA*, is a member of the trimeric class [14]. This class includes the human (HsPNP) and bovine homologues, among others. PNPs belonging to the trimeric class differ significantly from the hexameric class, which is usually present in prokaryotes [13][15][16]. The mycobacterial homologue is more specific to natural 6-oxopurine nucleosides (inosine, deoxyinosine, guanosine, and deoxyguanosine (2dGuo)) and synthetic compounds, and does not catalyze adenosine phosphorolysis [17]. This substrate specificity is in agreement with the concept that homotrimeric PNP enzymes cannot catalyze phosphorolysis and/or synthesis of 6-aminopurine nucleosides to an appreciable extent [18][19]. Although MtPNP has been numbered among the top 100 persistence targets by the TB Structural Genomics Consortium (www.webtb.org), its physiological role in *M. tuberculosis* remains to be demonstrated. Gene replacement experiments have been carried out to produce mutant strains defective in functional PNP. Surprisingly, *deoD*-encoded MtPNP appears to play an essential role in the survival of bacteria grown in rich medium, since a knockout strain could not be generated due to the unexpected essentiality of the gene (unpublished results). This result underscores the need for demonstrating protein function by experimental approaches instead of assigning function to a particular gene product based only on in comparative data.

II.3. Selective approach

A number of research groups have dedicated their efforts to determine specificity of substrates, kinetic mechanisms, and three-dimensional structures for PNPs from different bacterial sources [12][14][17][20]-[25] in comparison to HsPNP. Even though PNP activity is shared between humans and *M. tuberculosis*, drugs with selective toxicity against the mycobacterial enzyme can still be developed if one takes advantage of singular features that make them dissimilar [26]. In accordance with this proposal, it has recently been shown that even though bovine and human homologues share 87% sequence identity and have full conservation of the active site residues, inhibitors with differential specificity can be designed [27]. Although the mycobaterial and human homologues share 34.81% identity in amino acid sequence, the design of inhibitors with higher affinity for MtPNP seems to be feasible, since they appear to have different transition states [28] and structural features [25][29][30], which may be exploited to achieve specificity [24][31]-[39].

III. ENZYME KINETICS

MtPNP substrate specificity was probed by measurements of initial velocity employing natural and synthetic substrates [17]. The enzyme proved to be more specific for synthetic guanosine N7 methyl analogues, 2-amino-6-mercapto-7-methylpurine ribonucleoside (MESG) and 7-methylguanosine, than to natural nucleosides. This has been attributed to the increased catalytic constant values, since K_M values for all substrates were of similar magnitude. It is important to notice that the K_M value for MESG [17] was approximately 12-fold smaller than the one observed for HsPNP [39]. Indeed, the human homologue was shown to be more specific for natural substrates, such as inosine and guanosine, than to MESG [39]. These differences might imply that compounds with selective activity

against MtPNP may be developed based on chemical functional group substitutions of MESG, in particular the sulfur at the sixth position of the purine base.

Initial velocity, product inhibition, and equilibrium binding (spectrofluorimetry and surface plasmon resonance) data suggested that MtPNP catalyzes the phosphorolysis of 2dGuo by a steady-state ordered bi bi kinetic mechanism, in which inorganic phosphate (PO_4) is the first substrate to bind to the enzyme followed by 2dGuo binding to form the catalytically competent ternary complex, and R1P is the first product to dissociate from the enzyme followed by the dissociation of guanine (Gua) (Fig. 1).

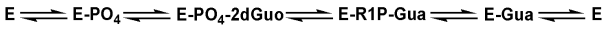

Fig. 1. Proposed enzyme kinetic mechanism for MtPNP with 2dGuo.

pH-rate profiles indicated a general acid as being essential for both catalysis and 2dGuo binding, and deprotonation of a group abolished phosphate binding. Proton inventory and solvent deuterium isotope effects indicated that a single solvent proton transfer makes a modest contribution to the rate-limiting step. Pre-steady-state kinetic data indicated that product release appears to contribute to the rate-limiting step for the MtPNP-catalyzed reaction [17].

IV. CRYSTALLOGRAPHIC STRUCTURE

IV.1. Overall structure description

MtPNP is composed predominantly of alanine (17.5%), leucine (12.3%), valine (10.1%), and glycine (10.4%) residues. As previously mentioned, PNPs with differing specificities have been identified, and, in a number of instances, purified from a broad range of organisms. Whereas most PNPs derived from bacteria are hexameric, MtPNP is a symmetrical homotrimer with a triangular arrangement of subunits similar to the mammalian PNP structures [24] (Fig. 2).

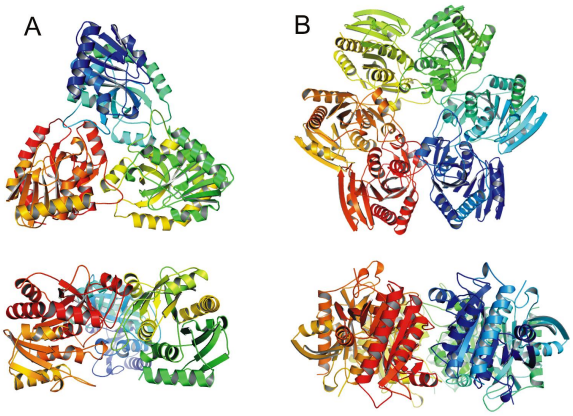

Fig. 2. Structures for (A) trimeric PNP (PDB: 1G2O) and (B) hexameric PNP (PDB: 1NW4).

In 2001, Wuxian Shi and co-workers solved, for the first time, the structures of MtPNP complexed with Immucillin-H (ImmH) and PO_4 and complexed with Iminoribitol, 9-deazahypoxanthine, and PO_4. These crystallographic structures were deposited on the Protein Data Bank (PDB) under the codes 1G20 and 1I80 [24], respectively. These structures provided a detailed picture of the catalytic conformation of MtPNP upon transition state binding.

Each monomer of the protein is folded into a single domain structure (α/β) containing nine β strands and nine α helices (Fig. 3). The core consists of a mixed eight-stranded β sheet (β2, Thr50-Gln54; β3, Gly70-Ile77; β4, His80-Glu87; β1, Val30-Leu34; β5, Gln113-Leu124; β9, Gln222-Thr230; β6, Gln132-Leu142; and β7, Ala176-Leu183). β5 and β9 are extended and participate in a smaller five-stranded distorted β barrel (β9; β5; β8; Asp203-Gly206; β7; and β6). The β sheet core is flanked by several α helices on each side (α1, Pro8-Thr23; α2, Val42-Ala44; α3, Arg98-Tyr99; α4, Pro103-Ser110; α5, Pro162-Ser171; α6, Pro191-Leu200; α7, Val210-Ala219; α8, His243-Ala251; and α9, Thr255-Arg267). Note that all secondary structural elements described here were identified using the molecular modeling software SPBDV v.4.0 [40]. These secondary structural elements are linked by extended loops, a characteristic feature common to all PNP structures solved to date. The segment connecting β2 and β3 (residues Ala55-Ala69) presents a disordered loop in MtPNP:ImmH:PO_4, although the authors reported that this loop was built into clear electron density in the $F_o - F_c$ electron density map. However, if compared to other structures (3IOM [25], 1I80 [24], and MtPNP:hypoxanthine (to be published elsewhere)), this loop presents a high root mean squared deviation of 8.21 Å, 8.44 Å, and 8.23 Å, respectively. The residues from this loop do not interact directly with bound inhibitor or phosphate, but are involved in the orientation of side chains of

the residues in the catalytic sites [24].

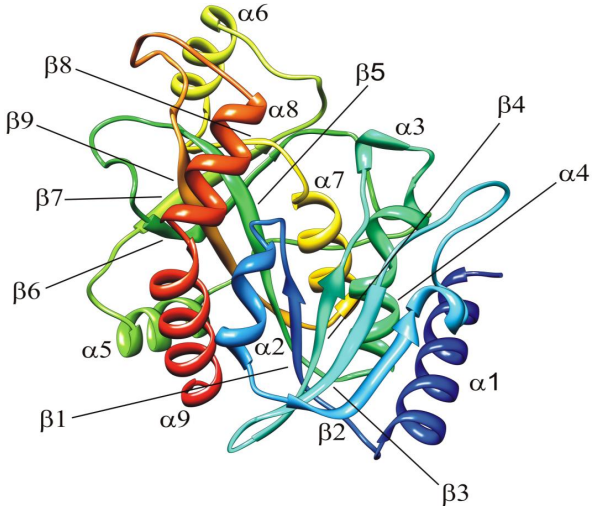

Fig. 3. Ribbon diagram of MtPNP showing the secondary structure (PDB: 3IOM).

Contacts between each subunit involve residues from Loop4 (Ala65), Loop5 (Tyr92-Glu93), β6 (Asp138-Leu142), Loop7 (Thr143-Ala159), β7 (Val179), Loop8-α6 (Pro184-Leu200), Turn (Met207), α7 (Ile214), and Loop9-α8 (Ala234-His243). The seven hydrogen bond interactions at the subunit interfaces include Tyr92(A) O-N Gly150(B), His187(A) ND1-OG Ser146(B), Tyr188(A) N-O Val154(B), Leu241(A) N-OD1 Asp155(B), Ala192(A) N-OD2 Asp138(B), Thr190(A) OG-O His139(B), and Glu193(A) OE2-N Asn141(B). The hydrophobic van der Waals interactions involve the pairs Tyr92(A)-Phe153(B), Tyr188(A)-Phe153(B), His243(A)-Phe153(B), His187(A)-Ile214(B), His187(A)-Leu156(B), Thr190(A)-Asp138(B), Thr190(A)-His139(B), Ala192(A)-Asp138(B), Glu193(A)-Leu140(B), and Met196(A)-Leu142(B).

In the trimeric PNPs, the entire active site is buried in the protein structure, and can be divided into three parts: the phosphate-binding site, in some crystallographic structures occupied by sulfate (used in high concentration in the crystallization conditions), and the pentose- and base-binding sites. The active site of each monomer is located in the interface of dimers. One active site in each dimer is located on the top and one on the bottom of the macromolecule. The distance between the active sites in each dimer is ~30 Å. At least two monomers are necessary to constitute a functional catalytic unit.

IV.2. Phosphate-binding site

The phosphate-binding site (Fig. 4C) is characterized by a cluster of positive charges comprised of Gly35, Ser36, His68, Arg88, His90, Tyr92, Asn119, Ala 120, and Ser208 residues. In MtPNP, most of these residues are in loops, except Asn119 and Ala120, which is part of β5, and Ser208, which is in a turn. All sulfate (phosphate) oxygen atoms form at least three intermolecular hydrogen bonds or salt bridges with the protein. The phosphate (sulfate) anion is also in contact with oxygen O3' and nitrogen N1' of the pentose ring moiety of ImmH (1G2O [24] and 1N3I [28]). No residues from the adjacent monomer interact with the phosphate-binding site as occurs in other organisms [13].

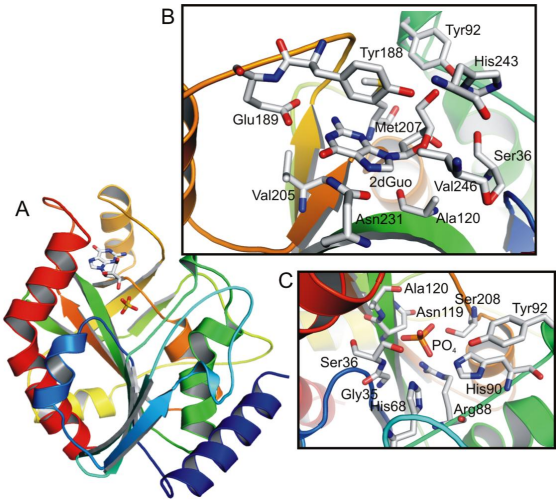

Fig. 4. Ligand-biding sites of MtPNP. (A) Monomer of MtPNP (PDB: 3IOM) complexed with sulfate and 2dGuo. (B) Pentose- and base-binding sites (PDB: 3IOM). (C) Phosphate-binding site (PDB: 1G2O).

Molecular dynamics simulations of the phosphate-binding site of *Plasmodium falciparum* PNP demonstrated that it is more stable than the purine-binding site [41], and could thus become an alternative site for the design of new inhibitors as observed for HsPNP [29].

IV.3. Pentose- and base-binding sites

Up to date, four crystallographic structures of MtPNP have been solved and deposited in PDB (1G2O [24], 1I80 [24], 1N3I [28], and 3IOM [25]). However, only 3IOM was solved in complex with a natural substrate. The pentose- and base-binding sites are located close to the phosphate-binding site, and share some amino acid residues, such as Ser36, Tyr92, Ala120, and Ser208. The structure of MtPNP in complex with sulfate and 2dGuo [25] gives a detailed view of the pentose- and base-binding sites. A number of hydrophobic residues are found in the base-binding site, such as Val205, Met207, and Val246. The amino acid residues in MtPNP pentose- and base-binding sites are shown in Fig. 4B. There are six intermolecular hydrogen bonds between the protein and 2dGuo, two between the pentose ring, and four with the base moiety. Hydrogen bond interactions with the sugar moiety involve Ser36 OG-O2 2dGuo and His243 ND1-O3

2dGuo; and Glu189 OE1-N4 2dGuo, Glu189 OE2-N5 2dGuo, Asn231 OD1-N3 2dGuo, and Asn231 OD2-O4 2dGuo with the guanine base moiety. However, in the structure of MtPNP:sulfate:2dGuo ternary complex, we did not observe the presence of Phe153 of adjacent subunit in the active binding site making hydrophobic contact and therefore no involvement in π-π interactions with the base moiety, as observed in other trimeric PNP-I enzymes [13].

IV.4. Structure-based drug design

Protein crystallography is an essential tool for the discovery and investigation of pharmacological interactions at the molecular level. The crystallographic structure of MtPNP provides valuable information for the structure-based design of antimycobacterial drugs, since it captures the features of an active binding site. However, it was shown that the pentose- and base-binding sites can accommodate molecular structures that are different from its natural substrates, so caution should be kept in mind when molecular docking simulations is carried out in order to find enzyme selective inhibitors [25]. The development of new potent selective inhibitors for MtPNP is still a scientific endeavor as they may present high toxicity, making them inappropriate for human administration. Accordingly, efforts to develop drugs with selective toxicity based on structural differences between MtPNP and HsPNP should be pursued. A number of research groups have thus included computational tools to achieve this goal.

V. POTENT INHIBITORS OF PNP

Potent inhibitors of PNPs are largely structural analogues of nucleoside substrates, embracing modifications of the base and/or pentose moiety, as well as replacement of the latter by other cyclic or acyclic moieties. The first structural changes only considered the ground state to the development of new inhibitors, obtaining IC_{50} values which ranged from 0.75 to 5 nM for PNP from mammalian erythrocytes [13]. The most outstanding molecule was 9-(3-pyridinyl-methyl)-9-deazaGua (BCX-34; Fig. 5), which is a potential candidate for the treatment of human T-cell proliferative disorders [42].

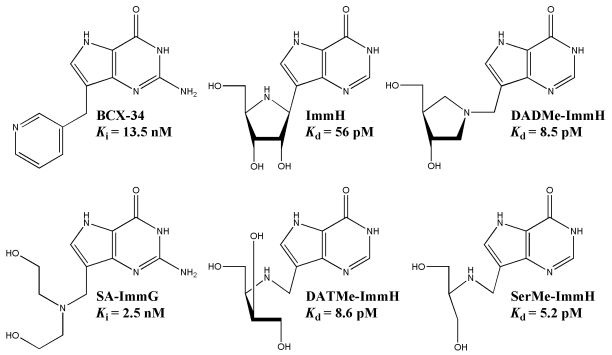

Fig. 5. Chemical structures of PNP inhibitors.

However the most potent inhibitors were designed from extensive kinetic isotope effect studies of transition states on the phosphorolysis reaction of inosine [43]. The first inhibitors based on the transition state structure were derived from (1*S*)-1-(9-deazahypoxanthin-9-yl)-1,4-dideoxy-1,4-imino-D-ribitol (ImmH; Fig. 5) and presented IC_{50} values ranging from 0.48 to 1.57 nM in mammalian hosts, including mice, monkeys, and humans. These compounds were further shown to be effective for T-cell selective immunosuppression, and clinical trials are ongoing [44]. It was also found that the inhibition mechanism is slow-onset, tight-binding with equilibrium dissociation constants (K_d) in the pM range (23 to 72 pM) [45].

As the transition state structures of PNPs-catalyzed phosphorolysis were determined, the Immucillin of second generation was synthesized, with K_d = 8.5 pM (DADMe-ImmH; Fig. 5). The structural changes were nitrogen atom by anomeric carbon, the ring oxygen by a methylene group to mimic the pentosyl moiety in the transition state. The 9-methylene bridge served to place the cationic N1' nitrogen near the ribosyl C1' position in the transition state and the 2'-hydroxyl group was removed to provide chemical stability [46]. Scaling up synthesis of DADME-ImmH has also been shown to be feasible [47].

In 2006, when seeking to simplify the Immucillin analogues, Corelli and co-workers [48] synthesized a series of acyclic Immucillin analogues (SA-ImmG; K_i = 2.5 nM; Fig. 5), which had a dissociation constant similar to the first generation of Immucillins. These acyclic derivatives made synthesis easy and low-cost which is fundamental to industrial scale-up. Based on these findings, an acyclic Immucillin series was further increased and the most active compound was DATMe-ImmH (Fig. 5). It was named third generation of PNP inhibitors with K_d = 8.6 pM [49].

More recently, a fourth generation of transition state analogues has been presented [50], of which the most active compound is SerMe-ImmH, with K_d = 5.2 pM (Fig. 5). It was demonstrated by

isothermal titration calorimetry studies that the conformationally flexible Immucillins reduced the system entropic penalty [51]. This inhibitor is structurally achiral, reducing the challenge for synthesis in large scale.

Regarding MtPNP, when only derivatives were evaluated, ImmH and DADMe-ImmH and their dissociation constants were 650 and 42 pM, respectively [28]. If we compare the transition states and substrate specificities of various PNPs, it appears to be possible to design species-specific inhibitors for use as therapeutic agents [52]. This seems feasible as we compare the K_i of HsPNP (56 pM) and MtPNP (650 pM). However, for DADMe-ImmH the difference is less pronounced: 16 pM for HsPNP and 42 pM for MtPNP. It has been proposed that changes in DADMe-ImmH are better to mimic the late transition state characteristic of the human enzyme catalyzed phosphorolysis [52].

VI. Conclusion

The present review strives to offer a brief review on current scientific data on MtPNP to provide insights on which to base selective drug development. As PNP-catalyzed phosphorolysis reaction is shared between humans and mycobacteria, differences in functional and structural features have been discussed to exploit them to achieve specificity.

Acknowledgements

This work was supported by funds of Millennium Initiative Program and National Institute of Science and Technology on Tuberculosis (INCT-TB), MCT-CNPq, Ministry of Health - Department of Science and Technology (DECIT) - Secretary of Health Policy (Brazil) to D.S.S., L.A.B and W.F.A.Jr. D.S.S. (CNPq, 304051/1975-06), L.A.B. (CNPq, 520182/99-5) and W.F.A.Jr. (CNPq, 300851/98-7) are Research Career Awardees of the National Research Council of Brazil (CNPq). R.G.D. and R.A.C. are postdoctoral fellows of CNPq.

References

[1] R.G. Ducati, A. Ruffino-Netto, et al., The resumption of consumption - a review on tuberculosis, *Memórias do Instituto Oswaldo Cruz, Volume 101,* (Issue 7), *November 2006, Pages 697-714.*

[2] R.G. Ducati, L.A. Basso, et al., Mycobacterial shikimate pathway enzymes as targets for drug design, *Current Drug Targets, Volume 8,* (Issue 3), *March 2007, Pages 423-435.*

[3] R.G. Ducati, A. Breda, et al., Purine Salvage Pathway in *Mycobacterium tuberculosis*, *Current Medicinal Chemistry, Accepted for publication, 2010.*

[4] A.D. Villela, Z.A. Sánchez-Quitian, et al., Pyrimidine Salvage Pathway in *Mycobacterium tuberculosis*, *Current Medicinal Chemistry, Accepted for publication, 2010.*

[5] Z.A. Sánchez-Quitian, C.Z. Schneider, et al., Structural and functional analyses of *Mycobacterium tuberculosis* Rv3315c-encoded metal-dependent homotetrameric cytidine deaminase, *Journal of Structural Biology, Volume 169,* (Issue 3), *March 2010, Pages 413-423.*

[6] S.T. Cole, R. Brosch, et al., Deciphering the biology of *Mycobacterium tuberculosis* from the complete genome sequence, *Nature, Volume 393,* (Issue 6685), *June 1998, Pages 537-544.*

[7] K. Duncan, Progress in TB drug development and what is still needed, *Tuberculosis (Edinburgh, Scotland), Volume 83,* (Issue 1-3), *2003, Pages 201-207.*

[8] H.M. Kalckar, Differential spectrophotometry of purine compounds by means of specific enzymes; determination of hydroxypurine compounds, *The Journal of Biological Chemistry, Volume 167,* (Issue 2), *February 1947, Pages 429-443.*

[9] A.K. Ojha, T.K. Mukherjee, et al., High intracellular level of guanosine tetraphosphate in *Mycobacterium smegmatis* changes the morphology of the bacterium, *Infection and Immunity, Volume 68,* (Issue 7), *July 2000, Pages 4084-4091.*

[10] T.P. Primm, S.J. Andersen, et al., The stringent response of *Mycobacterium tuberculosis* is required for long-term survival, *Journal of Bacteriology, Volume 182,* (Issue 17), *September 2000, Pages 4889-4898.*

[11] D.J. Porter, Purine nucleoside phosphorylase. Kinetic mechanism of the enzyme from calf spleen, *The Journal of Biological Chemistry, Volume 267,* (Issue 11), *April 1992, Pages 7342-7351.*

[12] C. Mao, W.J. Cook, et al., The crystal structure of *Escherichia coli* purine nucleoside phosphorylase: a comparison with the human enzyme reveals a conserved topology, *Structure, Volume 5,* (Issue 10), *October 1997, Pages 1373-1383.*

[13] A. Bzowska, E. Kulikowska, et al., Purine nucleoside phosphorylases: properties, functions, and clinical aspects, *Pharmacology & Therapeutics, Volume 88,* (Issue 3), *December 2000, Pages 349-425.*

[14] L.A. Basso, D.S. Santos, et al., Purine nucleoside phosphorylase from *Mycobacterium tuberculosis*. Analysis of inhibition by a transition-state analogue and dissection by parts, *Biochemistry, Volume 40,* (Issue 28), *July 2001, Pages 8196-8203.*

[15] K.F. Jensen, P. Nygaard, Purine nucleoside phosphorylase from *Escherichia coli* and *Salmonella typhimurium*. Purification and some properties, *European Journal of Biochemistry / FEBS, Volume 51,* (Issue 1), *February 1975, Pages 253-265*.

[16] K.F. Jensen, Two purine nucleoside phosphorylases in *Bacillus subtilis*. Purification and some properties of the adenosine-specific phosphorylase, *Biochimica et Biophysica Acta, Volume 525,* (Issue 2), *August 1978, Pages 346-356.*

[17] R.G. Ducati, D.S. Santos, et al., Substrate specificity and kinetic mechanism of purine nucleoside phosphorylase from *Mycobacterium tuberculosis*, *Archives of Biochemistry and Biophysics, Volume 486,* (Issue 2), *June 2009, Pages 155-164*.

[18] T.P. Zimmerman, N.B. Gersten, et al., Adenine as substrate for purine nucleoside phosphorylase, *Canadian Journal of Biochemistry, Volume 49,* (Issue 9), *September 1971, Pages 1050-1054*.

[19] J.D. Stoeckler, A.F. Poirot, et al., Purine nucleoside phosphorylase. 3. Reversal of purine base specificity by site-directed mutagenesis, *Biochemistry, Volume 36,* (Issue 39), *September 1997, Pages 11749-11756*.

[20] A. Bzowska, E. Kulikowska, et al., Properties of purine nucleoside phosphorylase (PNP) of mammalian and bacterial origin, *Zeitschrift für Naturforschung. C, Volume 45,* (Issue 1-2), *January-February 1990, Pages 59-70*.

[21] K.F. Jensen, Purine-nucleoside phosphorylase from *Salmonella typhimurium* and *Escherichia coli*. Initial velocity kinetics, ligand banding, and reaction mechanism, *European Journal of Biochemistry / FEBS, Volume 61,* (Issue 2), *January 1976, Pages 377-386*.

[22] J. Tebbe, A. Bzowska, et al., Crystal structure of the purine nucleoside phosphorylase (PNP) from *Cellulomonas sp.* and its implication for the mechanism of trimeric PNPs, *Journal of Molecular Biology, Volume 294,* (Issue 5), *December 1999, Pages 1239-1255*.

[23] T.H. Tahirov, E. Inagaki, et al., Crystal structure of purine nucleoside phosphorylase from *Thermus thermophilus*, *Journal of Molecular Biology, Volume 337,* (Issue 5), *April 2004, Pages 1149-1160*.

[24] W. Shi, L.A. Basso, et al., Structures of purine nucleoside phosphorylase from *Mycobacterium tuberculosis* in complexes with immucillin-H and its pieces, *Biochemistry, Volume 40,* (Issue 28), *July 2001, Pages 8204-8215*.

[25] R.G. Ducati, L.A. Basso, et al., Crystallographic and docking studies of purine nucleoside phosphorylase from *Mycobacterium tuberculosis*, *Bioorganic & Medicinal Chemistry, Volume 18,* (Issue 13), *July 2010, Pages 4769-4774*.

[26] W.B. Parker, M.C. Long, Purine metabolism in *Mycobacterium tuberculosis* as a target for drug development, *Current Pharmaceutical Design, Volume 13,* (Issue 6), *2007, Pages 599-608*.

[27] E.A. Taylor Ringia, P.C. Tyler, et al., Transition state analogue discrimination by related purine nucleoside phosphorylases, *Journal of the American Chemical Society, Volume 128,* (Issue 22), *June 2006, Pages 7126-7127*.

[28] A. Lewandowicz, W. Shi, et al., Over-the-barrier transition state analogues and crystal structure with *Mycobacterium tuberculosis* purine nucleoside phosphorylase, *Biochemistry, Volume 42,* (Issue 20), *May 2003, Pages 6057-6066*.

[29] L.F. Timmers, R.A. Caceres, et al., Structural studies of human purine nucleoside phosphorylase: towards a new specific empirical scoring function, *Archives of Biochemistry and Biophysics, Volume 479,* (Issue 1), *November 2008, Pages 28-38.*

[30] R.A. Caceres, L.F. Timmers, et al., Crystal structure and molecular dynamics studies of human purine nucleoside phosphorylase complexed with 7-deazaguanine, *Journal of Structural Biology, Volume 169,* (Issue 3), *March 2010, Pages 379-388*.

[31] W.F. de Azevedo Jr., F. Canduri, et al., Crystal structure of human purine nucleoside phosphorylase at 2.3Å resolution, *Biochemical and Biophysical Research Communications, Volume 308,* (Issue 3), *August 2003, Pages 545-552*.

[32] W. Filgueira de Azevedo Jr., F. Canduri, et al., Structural basis for inhibition of human PNP by immucillin-H, *Biochemical and Biophysical Research Communications, Volume 309,* (Issue 4), *October 2003, Pages 917-922*.

[33] W. Filgueira de Azevedo Jr., G.C. dos Santos, et al., Docking and small angle X-ray scattering studies of purine nucleoside phosphorylase, *Biophysical Research Communications, Volume 309,* (Issue 4), *October 2003, Pages 923-928*.

[34] W.F. de Azevedo Jr., F. Canduri, et al., Crystal structure of human PNP complexed with guanine, *Biophysical Research Communications, Volume 312,* (Issue 3), *December 2003, Pages 767-772*.

[35] F. Canduri, D.M. dos Santos, et al., Structures of human purine nucleoside phosphorylase complexed with inosine and ddI, *Biophysical Research Communications, Volume 313,* (Issue 4), *January 2004, Pages 907-914*.

[36] F. Canduri, V. Fadel, et al., Crystal structure of human PNP complexed with hypoxanthine and sulfate ion, *Biophysical Research Communications, Volume 326,* (Issue 2), *January 2005, Pages 335-338*.

[37] F. Canduri, V. Fadel, et al., New catalytic mechanism for human purine nucleoside phosphorylase. *Biophysical Research Communications, Volume 327,* (Issue 3), *February 2005, Pages 646-649*.

[38] D.M. dos Santos, F. Canduri, et al., Crystal structure of human purine nucleoside phosphorylase complexed with acyclovir. *Biophysical Research Communications, Volume 308,* (Issue 3), *August 2003, Pages 553-559.*

[39] R.G. Silva, J.H. Pereira, et al., Kinetics and crystal structure of human purine nucleoside phosphorylase in complex with 7-methyl-6-thio-guanosine, *Archives of Biochemistry and Biophysics, Volume 442,* (Issue 1), *October 2005, Pages 49-58*.

[40] N. Guex, M.C. Peitsch, SWISS-MODEL and the Swiss-PdbViewer: an environment for comparative protein modeling, *Electrophoresis, Volume 18,* (Issue 15), *December 1997, Pages 2714-2723*.

[41] F.B. Zanchi, R.A. Caceres, et al., Molecular dynamics studies of a hexameric purine nucleoside phosphorylase, *Journal of Molecular Modeling, Volume 16,* (Issue 3), *March 2010, Pages 543-550*.

[42] S. Bantia, J.A. Montgomery, et al., *In vivo* and *in vitro* pharmacologic activity of the purine nucleoside phosphorylase inhibitor BCX-34: the role of GTP and

dGTP, *Immunopharmacology, Volume 35,* (Issue 1), *October 1996, Pages 53-63*.

[43] P.C. Kline, V.L. Schramm, Purine nucleoside phosphorylase. Inosine hydrolysis, tight binding of the hypoxanthine intermediate, and third-the-sites reactivity, *Biochemistry, Volume 31,* (Issue 26), *July 1992, Pages 5964-5973*.

[44] S. Banti, P.J. Miller, et al., Comparison of *in vivo* efficacy of BCX-1777 and cyclosporin in xenogeneic graft-vs.-host disease: the role of dGTP in antiproliferative action of BCX-1777, *International Immunopharmacology, Volume 2,* (Issue 7), *June 2002, Pages 913-923*.

[45] R.W. Miles, P.C. Tyler, et al., One-third-the-sites transition-state inhibitors for purine nucleoside phosphorylase, *Biochemistry, Volume 37,* (Issue 24), *June 1998, Pages 8615-8621*.

[46] G.B. Evans, R.H. Furneaux, et al., Synthesis of second-generation transition state analogues of human purine nucleoside phosphorylase, *Journal of Medicinal Chemistry, Volume 46,* (Issue 24), *November 2003, Pages 5271-5276*.

[47] V.P. Kamath, J.J. Juarez-Brambila, et al., Development of a Practical Synthesis of a Purine Nucleoside Phosphorylase Inhibitor: BCX-4208, *Organic Process Research & Development, Volume 13,* (Issue 5), *July 2009, Pages 928-932*.

[48] T. Semeraro, A. Lossani, et al., Simplified analogues of immucillin-G retain potent human purine nucleoside phosphorylase inhibitory activity, *Journal of Medicinal Chemistry, Volume 49,* (Issue 20), *October 2006, Pages 6037-6045*.

[49] K. Clinch, G.B. Evans, et al., Third-generation immucillins: syntheses and bioactivities of acyclic immucillin inhibitors of human purine nucleoside phosphorylase, *Journal of Medicinal Chemistry, Volume 52,* (Issue 4), *February 2009, Pages 1126-1143*.

[50] M.C. Ho, W. Shi, et al., Four generations of transition-state analogues for human purine nucleoside phosphorylase *Proceedings of the National Academy of Sciences of the United States of America, Volume 107,* (Issue 11), *March 2010, Pages 4805-4812*.

[51] A.A. Edwards, J.M. Mason, et al., Altered enthalpy-entropy compensation in picomolar transition state analogues of human purine nucleoside phosphorylase, *Biochemistry, Volume 48,* (Issue 23), *June 2009, Pages 5226-5238*.

[52] E.A. Taylor Ringia, V.L. Schramm, Transition states and inhibitors of the purine nucleoside phosphorylase family, *Current Topics in Medicinal Chemistry, Volume 5,* (Issue 13), *2005, Pages 1237-1258*.

AUTHORS' INFORMATION

[1]Centro de Pesquisas em Biologia Molecular e Funcional (CPBMF), Instituto Nacional de Ciência e Tecnologia em Tuberculose (INCT-TB), Pontifícia Universidade Católica do Rio Grande do Sul (PUCRS), Porto Alegre, RS, Brazil.

[2]Faculdade de Biociências, Instituto Nacional de Ciência e Tecnologia em Tuberculose (INCT-TB), Laboratório de Bioquímica Estrutural, Pontifícia Universidade Católica do Rio Grande do Sul (PUCRS), Porto Alegre, RS, Brazil.

[*]Corresponding authors: Postal address: Centro de Pesquisas em Biologia Molecular e Funcional (CPBMF), Instituto Nacional de Ciência e Tecnologia em Tuberculose (INCT-TB), Pontifícia Universidade Católica do Rio Grande do Sul (PUCRS), Avenida Ipiranga 6681/92-A, 90619-900, Porto Alegre, RS, Brazil. Phone/Fax: +55-51-33203629. E-mail addresses: diogenes@pucrs.br (Diógenes S. Santos) or luiz.basso@pucrs.br (Luiz A. Basso).

Dr. Diógenes S. Santos was born in Gandu (Bahia State) in Brazil on June 28th, 1942. Dr. Santos did BSc in Veterinary Medicine at Federal University of Bahia (1968) in Brazil, MSc in Microbiology and Immunology at Federal University of São Paulo (1972), PhD awarded by Federal University of São Paulo (1975) for his experimental work at Medical Center of New York University (under Dr. Werner K. Maas supervision) in USA, and post-doc at Oxford University in England (1993-1995). Dr. Santos was adjunct professor at Federal University from to 1975 to 2003, and he is since full professor at Pontifical Catholic University of Rio Grande do Sul. The major field of study of Dr. Santos is the rational-drug design (function- and structure-based) of chemotherapeutic agents to treat tuberculosis and T-cell mediated diseases.

He has published over 129 papers in important international scientific journals (for instance, EMBO Journal, Cell, Molecualr Microbiology, Journal of Cellular Biochemistry, Infection and Immunity, Biochemistry-USA, Journal of Molecular Biology, Journal of Bacteriology, ABB, BBRC, Proteins, Biophysical Journal, Chemical Communications, Current Pharmaceutical Design, Bioorganic & Medicinal Chemistry, Journal of Structural Biology, Current Pharmaceutical Biotechnology, Current Drug Targets, Cell Biochemistry and Biophysics, Microbial Cell Factories, Acta Crystallographica, Journal of Inorganic Biochemistry, Tetrahedron Letters, Organic Letters, Protein Expression and Purification, Journal of Clinical Microbiology, MIOC, FEMS Microbiology Letters, Medicinal Chemistry Reviews, Avian Diseases). He has also published 9 book chapters and deposited over 31 structural coordinates on the Protein Data Bank (www.rcsb.org). He acted as mentor of 36 MSc dissertations and 8 PhD theses. Dr. Santos has filed for 4 patents in Brazil and 2 abroad (Patent Convention Treaty – PCT).

Dr. Santos was the founder, and director for ten years, of Biotechnology Center of Federal University of Rio Grande do Sul, and acted as consultant for BID, FAO and WHO. As co-ordinator of a program for graduate training of young brazilian scientists, Dr. Santos has masterminded the graduation of over 40 (forty) students abroad (from Japan, Europe, to California in USA). Dr. Santos is the Chief Executive Officer of "Quatro G Research & Development", a biotechnology-based private company. Dr. Santos is currently the head of the National Institute of Science and Technology on Tuberculosis of the Ministry of Health and Ministry of Science and Technology of Brazil.

Capítulo 6

Crystal structure and molecular dynamics studies of purine nucleoside phosphorylase from *Mycobacterium tuberculosis* associated with acyclovir

Artigo publicado no Biochimie

Capítulo 7

Combining crystallographic, thermodynamic, and molecular dynamics studiesof *Mycobacterium tuberculosis purine* nucleoside phosphorylase

Artigo a ser sumetido ao Journal of Molecular Biology

Combining crystallographic, thermodynamic, and molecular dynamics studies of *Mycobacterium tuberculosis* purine nucleoside phosphorylase

Rafael A. Caceres[a,b], Luís F. S. M. Timmers[a,c], Rodrigo G. Ducati[d], Leonardo A. Rosado[b,d], Luiz A. Basso[b,c,d], Diógenes S. Santos[b,c,d], Walter F. de Azevedo Jr.[a,b,c,*]

[a] Faculdade de Biociências, Laboratório de Bioquímica Estrutural, Pontifícia Universidade Católica do Rio Grande do Sul, Porto Alegre, RS, Brazil - Instituto Nacional de Ciência e Tecnologia em Tuberculose (INCT-TB).

[b] Programa de Pós-Graduação em Medicina e Ciências da Saúde, Pontifícia Universidade Católica do Rio Grande do Sul, Porto Alegre, RS, Brazil.

[c] Programa de Pós-Graduação em Biologia Celular e Molecular, Pontifícia Universidade Católica do Rio Grande do Sul, Porto Alegre, RS, Brazil.

[d] Centro de Pesquisas em Biologia Molecular e Funcional, Instituto de Pesquisas Biomédicas, Pontifícia Universidade Católica do Rio Grande do Sul, Porto Alegre, RS, Brazil - Instituto Nacional de Ciência e Tecnologia em Tuberculose (INCT-TB).

[*]Corresponding author:
Walter Filgueira de Azevedo Jr.
Av. Ipiranga, 6681, CEP 90619-900, Porto Alegre, RS, Brazil
walter@azevedolab.net
Telephone: +55 51 33534529

Abstract

Purine nucleoside phosphorylase (PNP) plays a central role in purine metabolism, normally operating in the purine salvage pathway of cells. This paper presents the crystallographic structure of MtPNP associated with inosine and hypoxanthine, substrate and product, respectively. In addition, dynamics simulations and isothermal titration calorimetry were performed to provide detailed information on the dynamic properties, and to investigate the thermodynamic profile and affinities, respectively, of MtPNP associated with substrate and product.

Keywords: Tuberculosis, Purine nucleoside phosphorylase, Crystallographic structure, Molecular dynamics, Isothermal titration calorimetry.

Introduction

Human tuberculosis (TB), caused by *Mycobacterium tuberculosis*, is a ubiquitous, highly contagious chronic granulomatous bacterial infection which is still a leading killer of young adults worldwide. Susceptibility to TB in HIV-infected populations represents a serious health problem throughout the world. Furthermore, during the last decade, multidrug-resistant TB has been increasing in incidence not only in developing countries but in industrialized nations as well. Currently, one third of the world's population is infected with *M. tuberculosis* (Ducati et al., 2004; Nunn et al., 2005). These data strongly indicate the importance for the development of new anti-TB agents, capable of shortening duration of treatment, reducing the total number of doses, and/or being active against latent bacteria, which would contribute to the effective control of this disease, particularly in developing countries.

Homologues to enzymes of essential pathways have been identified in the *M. tuberculosis* genome sequence (Cole et al., 1998; Ducati et al., 2007; Ducati et al. 2010b; Villela et al., 2010). Purine nucleoside phosphorylase (PNP; EC 2.4.2.1) is a key enzyme of the purine salvage pathway, responsible for the inter-conversion between (deoxy)nucleosides and bases, which in turn may be converted to uric acid for excretion or reused in nucleic acid biosynthesis (Ducati et al., 2010b; Parks and Agarwal, 1972). This enzyme catalyzes the reversible cleavage, in the presence of inorganic phosphate (P_i), of *N*-glycosidic bonds of purine β-(deoxy)nucleosides, except adenosine, to generate α-(deoxy)ribose 1-phosphate and the corresponding purine base (Ducati et al., 2009; Ducati et al., 2010c; Kalckar, 1947) (Fig. 1). Studies with mutants of the purine biosynthesis pathway have shown

reduction of the bacillus capacity to spread in mammalian hosts (Jackson et al., 1996).

In this work we describe, for the first time, the crystallographic structure of *M. tuberculosis* PNP (MtPNP) associated with either inosine (INO) or hypoxanthine (HX). These structures were refined at 1.99 Å and 1.95 Å, respectively, using recombinant MtPNP protein and Synchrotron radiation source. Here we also present molecular dynamics (MD) simulations to provide detailed information on the dynamic properties of the crystallographic structures in solution. Furthermore, isothermal titration calorimetry (ITC) revealed different thermodynamic profiles and affinities between the enzyme and INO and HX. All these analyses could give support to enhance the knowledge on this enzyme, providing new insights into interacting chemical groups in MtPNP enzyme active site. In this context, the understanding of enzymes involved in purine metabolism could enable directional design of potent and selective inhibitors of *M. tuberculosis* growth.

Materials and Methods

Crystallization and data collection

MtPNP:INO:SO_4 and MtPNP:HX were crystallized using the experimental conditions described elsewhere (Basso et al., 2001;; Ducati et al., 2010a; Shi et al., 2001). PNP solution was concentrated to 25 mg/mL and co-crystallized with INO:SO_4 and HX. Hanging drops were prepared mixing 1 μL of protein solution and 1 μL of reservoir solution (100 mM Tris pH 8.0 25 % PEG3350 25 mM $MgCl_2$). The crystals were flash frozen at 100 K. X-ray diffraction data were collected at 1.431 Å wavelength using Synchrotron

Radiation Source (Laboratório Nacional de Luz Síncrotron, Campinas, SP, Brazil) and a CCD detector (MARCCD). The data were processed using Mosflm and scaled with Scala (Collaborative Computational Project Number 4, 1994) programs.

Structure resolution and refinement

The crystal structures of MtPNP:INO:SO_4 and MtPNP:HX were determined by standard molecular replacement using the AMoRe software (Navaza, 1994) and the structure of MtPNP in complex with 2-deoxyguanosine and sulfate (PDB code: 3IOM (Ducati et al., 2010a)) as template. Structure refinement was performed using the Refmac5 software (Collaborative Computational Project Number 4, 1994). The atomic positions obtained from molecular replacement were used to initiate the crystallographic refinement. The overall stereochemical quality of the final model was assessed by the Procheck software (Laskowski et al., 1993).

Molecular dynamics simulations

The crystallographic data revealed that the asymmetric unit contains two protomers although the trimer is generated by the symmetry elements from the protomers in different asymmetric units. Molecular dynamics (MD) simulations were performed with the trimeric structure of the MtPNP to provide a more realistic analysis, since the MtPNP is biologically active as a trimer (Ducati et al., 2010a). All MD simulations were carried out using the GROMACS 4.0.5 package (van der Spoel et al., 2005) with the 96.1 (53a6) GROMOS force field. MD simulations for the enzyme with INO bound (PDB

access code: 3IX5) and HX (PDB access code:3SCZ) were performed to investigate the dynamic nature of the interactions between the protein-ligand complexes and water molecules.

The MD simulations were carried out using the particle mesh Ewald method (Darden et al., 1993) for the electrostatic interactions. The van der Waals and Lennard-Jones interaction were evaluated using a 14.0 Å and 10.0 Å atom-based cutoff, respectively. The integration time step was 2.0 fs, with the neighbor list being updated every ten steps by using the grid option and a cutoff distance of 12.0 Å. The simple point charge extended (SPC/E) (Barendsen et al., 1981) water model was used. Periodic boundary condition has been used with constant number of particles, pressure, and temperature (NPT) in the system. The V-rescale thermostat was applied using a coupling time of 0.1 ps to maintain the systems at a constant temperature of 310 K. The Berendsen barostat was used to maintain the systems at a pressure of 1 bar, and values of the isothermal compressibility were set to 4.5×10^{-5} bar^{-1} for water simulations. The temperature of the systems were increased from 50 K to 300 K in five steps (50-100, 100-150, 150-200, 200-250, and 250-300 K), and the velocities at each step were reassigned according to the Maxwell-Boltzmann distribution at that temperature and equilibrated for 10 ps, except for the last part of the thermalization phase, which was of 20 ps. The systems were submitted to a steepest descent followed by conjugate gradient energy minimizations up to a tolerance of 1,000 kJ/mol. A MD simulation with position restraints was carried out for a period of 20 ps in order to allow the accommodation of the water molecules in the system. Finally, 20 ns MD simulations were performed to all systems. The topology files and other force field parameters, except the charges of ligands, were generated using the

PRODRG program (van Aalten et al., 1996). The partial atomic charges to the ligands were calculated using the ChelpG method (Breneman and Wiberg, 1990), available in the Gaussian03 package (Frisch et al., 2003), being submitted to single-point ab initio calculations at DFT/B3LYP/6-31G** level.

Essential dynamics

Protein functions are embedded in their structure and a major goal of protein simulation is to generate enough configurations of the system of interest to extract functionally relevant motions. One such tool for reducing the generated dimensionality of a MD trajectory to an essential subspace encompassing few degrees of freedom, eliminating the positional fluctuations, is essential dynamics (ED), also known as principal component analysis (Amadei et al., 1993). ED is a method commonly used for dissecting the dynamics of proteins and their importance in biological processes, like protein folding or substrate binding. The ED analysis is a technique that reduces the complexity of the data and extracts the concerted motion in simulations that are essentially correlated and presumably meaningful for biological function (Mascarenhas et al., 2010). In the ED analysis, a variance/covariance matrix was constructed from the trajectories after removal of the rotational and translational movements. A set of eigenvectors and eigenvalues was identified by diagonalizing the matrix. The eigenvalues represent the amplitude of the eigenvectors along the multidimensional space, and the displacements of atoms along each eigenvector show the concerted motions of protein along each direction. An assumption of ED analysis is that the correlated motions for the function of the protein are described by eigenvectors with large eigenvalues. The protein movements in the essential subspace were identified

by projecting the Cartesian trajectory coordinates along the most important eigenvectors from the analysis. ED was performed using analysis tools from the GROMACS package, considering only the backbone atoms for generating the covariance matrix. Prior to performing ED, all translations and rotational motions were eliminated by fitting the trajectory to a reference structure, in this case, the average structure.

Isothermal titration calorimetry

ITC experiments were carried out using an iTC_{200} Microcalorimeter (Microcal, Inc., Northampton, MA). Calorimetric experiments were carried out with either INO or HX at 25 °C. For experiments with the substrate, the sample cell (200 µL) was filled with MtPNP at a concentration of 99 µM and 5 mM sulfate, and the injection syringe (39 µL) was filled with 2 mM INO. For experiments with the product, the sample cell (200 µL) was filled with MtPNP at a concentration of 92 µM, and the injection syringe (39 µL) was filled with 1 mM HX. The reference cell (200 µL) was loaded with water during all experiments, and all measurements were carried out in 50 mM Tris pH 7.6. The binding reaction started with one injection of 0.5 µL of ligand followed by 10 injections of 3.9 µL at intervals of 180 s, reaching a final volume 39.5 µL with a stirring speed of 500 RPM. The heat variation was monitored inside the cell allowing determination of binding enthalpy (ΔH) of the process and association constant at equilibrium (K_a).

Control titrations were performed to subtract the heats of dilution and mixing for each experiment. The Gibbs free energy (ΔG) of binding was calculated using the relationship described in Eq. (1), in which R is the gas

constant (8.314 J K^{-1} mol^{-1}), *T* is the temperature in Kelvin (T = °C + 273.15), and K_a is the association constant at equilibrium. The entropy of binding (*ΔS*) can also be determined by Eq. 1. One set of sites model was utilized to determine the binding and thermodynamic constants. Estimates for K_a and Δ*H* parameters were refined by standard Marquardt nonlinear regression method provided in the Origin 7 SR4 software. Entropy values are described as -*T ΔS*.

$$\Delta G^o = -RT \ln K_a = \Delta H^o - T\Delta S^o \quad (1)$$

Results and discussions

Molecular replacement and crystallographic refinement

The MtPNP:INO:SO_4 and MtPNP:HX structures were solved by molecular replacement with the AMoRe software (Navaza, 1994) using the crystallographic structure of MtPNP associated to 2-deoxyguanosine and sulfate (PDB code: 3IOM (Ducati et al. 2010a) as a template. The crystals diffracted to 1.99 Å (MtPNP:INO:SO_4) and 1.95 Å (MtPNP:HX) resolution and belong to orthorhombic space group H3. Model buildings were performed with the MIFiT 3.1.0 program (McRee, 2004) using F_{obs} - F_{calc} and $2F_{obs}$ - F_{calc} density maps that show the electron density for the INO, SO_4, and HX in the structures (Fig. 2). Atomic coordinates for INO, SO_4, and HX ions have been included in the model and all crystallographic refinement using Refmac5 (Collaborative Computational Project Number 4, 1994) continued with maximum likelihood protocol, followed by alternate cycles of positional refinement and manual rebuilding using MIFit 3.1.0 (McRee, 2004). A total of

269 (MtPNP:INO:SO_4) and 280 (MtPNP:$HX_)$ water molecules were added to the models. The final model had R_{free} and R_{factor} of 23.53 and 18.04% to MtPNP:INO:SO_4, and 17.57% and 22.57% to MtPNP:HX, respectively. The correlation coefficients to MtPNP:INO:SO4 and MtPNP:HX were 98.73% and 100%, respectively. The highest magnitude of the correlation coefficient function obtained for the Euler angles to MtPNP:INO:SO_4 were α = 29.32°, β = 97.93°, and γ = 6.57°, and to MtPNP:HX were α = 90.56°, β = 82.17°, and γ = 186.66°. The fractional coordinates to MtPNP:INO:SO_4 are T_x = 0.2360, T_y = 0.4560, and T_z = 0, and to MtPNP:HX are Tx = 0.1233, Ty = -0.4308, and Tz = 0. Data collection and structure refinement are summarized in **Table 1.**

Analysis of the Ramachandran diagram ϕ - ψ for the structure indicates that 90.70% of residues are in the most favored regions, 8.10% in the additional allowed regions, 0.70 % in the generously allowed regions, and 0.50% in the disallowed regions of the plot for MtPNP:INO:SO_4, and 91.20% of residues are in the most favored regions, 7.90% in the additional allowed regions, 0.50% in the generously allowed regions, and 0.50% in the disallowed regions of the plot for MtPNP:HX. Analysis of the electron density map ($2F_{obs}$ - F_{calc}) agrees with the Ala65 to Ala69 of the three subunits, positioning this same residues in the disallowed regions in the other MtPNP structures previous solved (Nolasco et al., 2004).

Overall crystallographic structure of MtPNP:INO:SO_4 and MtPNP:HX

These complexes follow a trimeric arrangement similar that previously described for mammalian and mycobacterial PNPs (Basso et al., 2001; de Azevedo Jr., 2008; Caceres et al., 2010; Ducati et al., 2010a; Nolasco et al.,

2004; Shi et al., 2001; Timmers et al., 2008;). Each subunit is folded into an α/β fold consisting of nine α-helices surrounded by nine β-sheets (Fig. **3**). MtPNP:INO:SO_4 and MtPNP:HX structures present an electron density in the classical binding site, clearly suggesting the presence of INO and HX, respectively. All interactions analysis between the product and substrate with the MtPNP were evaluated with the PISA v.1.20 program (Krissinel and Henrick, 2007).

MtPNP in complex with INO (substrate) shows one hydrogen bond (HB), between the δ-guanido group of Asn231 and the 6-carbonyl oxygen of INO. Three HBs were observed in the ribose moiety (O2*, O3*, and O5*), and the fourth on the purine moiety (Fig. 4A). In addition, eighteen van der Waals interactions between INO and the residues Ser36, Arg88, His90, Tyr92, Asn119, Ala120, Ala121, Gly122, Tyr180, Tyr188, Glu189, Val205, Gly206, Met207, Ser208, Thr230, Ala233, Leu241, His243, and Val246 were observed, contributing to the ligand stabilization into the binding site. Knowing the ribose moiety flexibility, almost all these hydrophobic interactions are driven to increase the stability or this portion. Furthermore, taking into account the residues buried percentage area, it was observed that nine (Asn119, Ala121, Gly122, Tyr180, Val205, Gly206, Thr230, Ala233, and Val246) of those eighteen residues remain 40% or more buried into the binding site, suggesting its importance to substrate recognition.

MtPNP in complex with HX (product) presented three HBs, involving Glu189 (OE1) and Asn231 (ND2 and OD1) with HX (N1, N7, and O6) (Fig. 4B). Eleven hydrophobic interactions involving Ala120, Ala121, Gly122, Tyr188, Val205, Gly206, Met207, Thr230, Ala233, Leu241, and Val246 residues were observed in the structure. Keeping in mind the residues buried

percentage area concept, seven of those eleven residues involved in hydrophobic interactions remain 40% or more into the binding site (Ala120, Ala121, Ala122, Val205, Gly206, Thr230, and Val246). Furthermore, comparing the interactions between MtPNP:INO:SO_4 and MtPNP:HX, it was observed that when the structure is in complex with the substrate, the residues orientation allow an active site organization due to the increased number of residues buried into the binding pocket.

Analysis of the subunit interfaces between MtPNP:INO:SO_4 and MtPNP:HX show that the former structure presents six HBs involving residues Asn141(B)-Glu193(A), Asp138(B)-Ala192(A), His139(B)-Thr190(A), Ser146(B)-His187(A), Val154(B)-Tyr188(A), and Asp155(B)-Leu241(A). All these HB interactions were also observed in the structure associated with HX. The hydrophobic interaction was also monitored, presenting 42 interactions to MtPNP:INO:SO_4 and 41 interactions to MtPNP:HX. In addition, both structures shared twelve strategic residues (Tyr92, Leu140, Thr143, Leu148, Phe153, Thr157, Val157, Gly185, Pro191, Met196, Ile214, and Ala234), which could be relevant to the trimeric structure stability.

Regarding the importance of the quaternary structure to MtPNP biological activity, we monitored which residues were often related to the steady trimeric structure taking into account all MtPNPs previously published (Ducati et al., 2010a; Lewandowicz et al., 2003). The residues identified as being important for MtPNP trimeric structure organization are Leu140, Thr143, Phe153, Val179, Gly185, Pro191, Met196, Ile214, and Ala234. These residues are approximately 60% buried into the adjacent subunit, and could allow the quaternary structure maintenance. Considering these interface residues, Phe153 caught our attention, since, in the human PNP this same

residue (Phe159) presents an important role in the ligand stabilization process, which was identified making hydrophobic interactions with the adjacent binding site. However, analyzing this residue in MtPNP, we observed no interaction between Phe153 and the adjacent binding site. This finding may be due to differences between the length of polypeptide chains, where human PNP presents 21 amino acids more than MtPNP, allowing an approximation of Phe159 to the active site.

Molecular dynamics simulations

The MD simulations of MtPNP:INO:SO_4 and MtPNP:HX ternary complex structures were performed using SPC/E water model, as previously mentioned, applying periodic boundary conditions, and using the MtPNP trimeric form, aiming to mimic the biological organization found in nature. The stability of the quaternary structure during the MD simulations was assessed by the radius of gyration (Rg) and the root mean square deviation (RMSD). Rg and RMSD as a function of time are shown in Fig. 5. The mean values of the Rg averaged over the period from 5 to 20 ns were determined, giving 28.18 ± 0.12 Å and 28.07 ± 0.14 Å for MtPNP:INO:SO_4 and MtPNP:HX, respectively. The mean values of the RMSD averaged over the period from 5 to 20 ns were determined, giving 2.76 ± 0.28 Å and 2.19 ± 0.19 Å for MtPNP:INO:SO_4 and MtPNP:HX, respectively. Rg and RMSD remained essentially constant after 5000 ps for both systems, suggesting that the molecular conformation was significantly preserved as a whole. This analysis suggests that Rg centered on the center of mass of the trimeric MtPNP remains essentially constant, indicating that the monomers of MtPNP structure remain in the trimeric state, which is the biological unit for MtPNP.

The total interaction energies of both systems versus simulation time are shown in Fig. 6, which gives an indication of the overall stability of the MD trajectory. In general, the total interaction energy of the simulations decreased slightly but did not change to a large extent during the simulation. The mean values of the total interaction energy averaged over the period from 5 to 20 ns were determined, giving -240.189 ± 22.73 kJ/mol and -141.242 ± 20.02 kJ/mol for MtPNP:INO:SO_4 and MtPNP:HX, respectively. It is interesting to highlight that the simulation of MtPNP in complex with INO presented lower total interaction energy when compared to MtPNP associated with HX. This finding is in agreement with what is expected, where the product presents a lower affinity by the protein allowing the release the equivalent purine base. However, should be noted that the analysis of interaction energy, here performed, between protein and solute (INO or Hx) only takes into account the non-bonded interactions, Lennard-Jones and Coulomb interactions terms, precisely. Leaving out the calculation of entropic effect and therefore the energy desolvation cost.

Essential dynamics

To consider only the prevalent protein motions during the MD simulation, and in order to identify peculiarities between MtPNP:INO:SO_4 and MtPNP:HX, ED analysis was carried out. We built the covariance matrices of the atomic fluctuations in a MD trajectory, in which the overall translation and rotation modes were removed. Elimination of the overall motion was done at each simulation step and the total removal of these irrelevant motions was ensured by fitting all the structures to the initial structure. It has been shown that it is sufficient to use only the Cα atomic positions when building the

covariance matrix (Hess, 2000). The matrix is built considering structures sampled every 0.5 ps from the production run of the simulations. A total of 262 residues were included in the analysis, and diagonalization of the covariance matrix resulted in 786 eigenvectors.

Table 2 shows the contribution to the overall motion of the first 10 eigenvectors of one singled-out simulation for each structure and the contribution from each subunit in the protein. It can be seen that the first 10 eigenvectors describe a representative percentage of the motions, 64.75% and 57.25% in average, for the trimeric MtPNP:INO:SO_4 and MtPNP:HX, respectively.

The analysis of the MtPNP:INO:SO_4 subunit simulation has shown that the total positional fluctuations described by the first 10 eigenvectors are 59.55%, 66.56%, and 68.14% for subunits A, B, and C, respectively. The results of the first eigenvectors alone represent 20.35% (subunit A), 33.73% (subunit), and 38.93% (subunit) of the total motion of the protein. For the MtPNP:HX complex simulation, the analysis has shown that the total positional fluctuations described by the first 10 eigenvectors are 56.59%, 59.89%, and 55.29% for subunits A, B, and C, respectively. The results of the first eigenvectors alone represent 19.76% (subunit A), 22.75% (subunit B), and 24.25% (subunit C) of the total motion of the protein (Table 2). The significant fluctuations of the first eigenvector are shown in Fig. 7. The main fluctuations are presented for the regions formed by loops and secondary structure unfolding (losses). We identified three main regions, R1, R2, and R3, which were analyzed separately for each subunit (A, B, and C). R1, composed by Ser36 to Phe60, does not present any significant change. The decreasing fluctuation observed when MtPNP is bounded to HX, may be nothing more

than a loop organization, and, in addition, this region is far away from the subunits interface or from the purine active site. R2, which is comprised by residues Ile136 to Tyr160, seems to be the same as for R1, a large loop region. However, analyzing a specific region in subunit A, which is composed by Arg145 to Gly150, we observed a large loop fluctuation. R3, which comprises Val246 to Leu260, is located near to the purine binding site, and presents residues that contributed with hydrophobic interactions to ligand stabilization. In the MtPNP:INO:SO_4 complex, this region presented a stable α-helix, which allows a better ligand accommodation into the active site. However, comparing this same region with MtPNP:HX complex, disorganization is clear, as the α-helix which once was stable when associated with a reaction product forms a loop, and an instability of the residues making hydrophobic interactions with the substrate is observed.

Isothermal titration calorimetry

ITC measurements were carried out to determine the thermodynamic interaction and affinity between the enzyme and the ligands. The formation of MtPNP:INO:SO_4 and MtPNP:HX complexes show significant heat changes, providing a thermodynamic signature of non-covalent interactions to each binding process. Interatomic interactions, such as hydrogen bonds and van der Waals, dictate the enthalpy pattern, where a positive enthalpy indicates a favorable net redistribution of the interaction between reacting species (O'Brien et al., 2004). The entropy nature is related to the degree of hydrophobic interactions upon complex formation reflecting on the disorder of bound and free molecules. Favorable entropy is associated to the release of

water molecules from the surface to the bulk and negative entropy is related to a conformational change in either ligand or protein (O'Brien et al., 2004).

MtPNP:SO_4:INO complex formation shows a favorable enthalpy (-4.0 ± 0.2 Kcal/mol) and entropy (6.36 ± 0.49 cal/mol/deg), resulting in a favorable Gibbs free energy (-5.9 ± 0.5 Kcal) and an equilibrium dissociation constant (K_D) of 47 ± 4 μM (Fig. 8A). The thermodynamic constants indicate a favorable redistribution of hydrogen bonds/van der Waals interactions and probably a release of "bound" water molecules to the bulk solvent, resulting in a favorable enthalpy/entropy and free Gibbs energy.

MtPNP:HX complex formation shows a large favorable enthalpy (-15.4 ± 0.1 Kcal/mol) and a negative entropy (-22.5 ± 3.3 cal/mol/deg), resulting in a large positive Gibbs free energy of (-8.6 ± 1.3 Kcal/mol) and a low K_D of 434 ± 64 nM (Fig. 8B). Incidentally, these results indicate a remarkable redistribution of hydrogen bonds/van der Waals interactions resulting in a large favorable enthalpy and a negative entropy value possibly due to a conformational change in either ligand or protein. Interestingly, the equilibrium dissociation constant and Gibbs free energy values indicate strong and spontaneous interaction process, even though the entropic contribution to binding was not favorable. Accordingly, the unfavorable entropy was off-set by the large favorable enthalpy.

Conclusions

The resolution of MtPNP structures in complex with either INO or HX provided an enrichment of structural information about active site peculiarities when MtPNP is associated with a substrate and a product, highlighting which

residues are frequently participating in the ligand interaction process. The main residues, Glu189 and Asn231, which interact with the ligands anchoring them into the binding site, were observed in MtPNP bounded to INO and HX. In addition, the residue Phe153, which in human PNP corresponds to Phe159, does not show the same importance to MtPNP due to differences between the number of residues in human PNP (289 amino acids) and MtPNP (268 amino acids), disallowing Phe153 presence into the binding pocket. Dissecting the MD results, it could be observed that the total interaction energy between MtPNP associated with INO and HX presented a significant difference. MtPNP:INO:SO_4 is 100 kJ/mol lower than MtPNP:HX. Considering that we are analyzing a substrate and a product, this difference is predictable, as it allows the product release. Furthermore, taking into account the ED results, it was possible to identify three regions (R1, R2, and R3), which were separately analyzed. R1 and R2 were identified as loop regions, which were far away from the binding pocket, and do not present any kind of interaction between the subunits interfaces. R3 comprises an α-helix, located in the MtPNP C-terminal, and, in MtPNP:HX, this region presented a loss of two turns of this α-helix when compared to MtPNP:INO:SO_4. Therewithal, the resolution of these MtPNP:INO:SO_4 and MtPNP:HX structures, and MD simulations may provide some clues as to which residues must be taken into consideration in the development of structure-based drug design initiatives, allowing an accurate inhibitor search focused on MtPNP. ITC is an important technology for drug discovery due to its capacity to determine, in a single experiment, the affinity and the thermodynamic profile between two molecules, which helps understand the conformational changes upon binary complex formation. The ITC values indicate a MtPNP preference for HX in the present assay

conditions, corroborating with enzyme activity assays (data not shown), where HX has a K_M and specificity constant more favorable than INO. Though unexpected, this result is consistent with the previous research data (Friedkin, 1950) indicating that thermodynamically, the equilibrium of the reaction is shifted in favour of nucleoside synthesis. Although, *in vivo*, the phosphorolysis is highly favoured over synthesis due to coupling with two additional enzymatic reactions, oxidation followed by the phosphoribosylation of the released purine base by xanthine oxidase and hypoxanthine-guanine phosphoribosyltransferase, respectively (Bzowska et al. 2000).

Occasionally conflicting results are obtained by different experimental techniques that could lead to misunderstanding of a biological system, and the application of different approaches should help. Indeed, our results highlights strikingly the importance of combination of different techniques in order to circumvent its limitations. For example, the crystallographic medium is capable to induce conformational changes in the protein by packing, not observed in biological environment, and the MD could help understanding the folding and structural patterns of macromolecules under solution.

Therefore, our results provide new data on which to base scientific knowledge on MtPNP towards selective drug development.

Deposit

The atomic coordinates and structure factors for the MtPNP:INO:SO_4 and MtPNP:HX structures have been deposited at the Protein Data Bank, access code: 3IX5 and 3SCZ, respectively.

Acknowledgments

This work was supported by the National Institute of Science and Technology on Tuberculosis (Decit/SCTIE/MS-MCT-CNPq-FNDCTCAPES). L.A.B., D.S.S., and W.F.A.Jr. also acknowledge financial support awarded by FAPERGS-CNPq-PRONEX-2009. D.S.S. (304051/1975-06), L.A.B. (520182/99-5), and W.F.A. Jr. (300851/98-7) are research career awardees of the National Council for Scientific and Technological Development of Brazil (CNPq). R.A.C and L.A.R acknowledges a scholarship awarded by CNPq. L.F.S.M.T. acknowledges a scholarship awarded by CAPES. R.G.D. is a postdoctoral fellow of CNPq.

References

Amadei, A., Linssen, A.B., Berendsen, H.J., 1993. Essential dynamics of proteins. Proteins. 17, 412-425.

Basso, L.A., Santos, D.S., Shi, W., Furneaux, R.H., Tyler, P.C., et al., 2001. Purine nucleoside phosphorylase from *Mycobacterium tuberculosis*. Analysis of inhibition by a transition-state analogue and dissection by parts. Biochemistry. 40, 8196-8203.

Berendsen, H.J.C., Postma, J.P.M., van Gunsteren, W.F., Hermans, J., 1981. Interaction models for water in relation to protein hydration. In: Pullman, B. (Ed.), Intermolecular Forces. D. Reidel Publishing Company, Netherlands.

Breneman, C.M., Wiberg, K.B., 1990. Determining atom-centered monopoles from molecular electrostatic potential. The need for high sampling density in formamide conformational analysis. J. Comput. Chem. 11, 361-373.

Bzowska, A., Kulikowska, E., Sugar, D., 2000. Purine nucleoside phosphorylases: properties, functions, and clinical aspects. Pharmacol. Ther. 88, 349-425.

Caceres, R.A., Timmers, L.F., Pauli, I., Gava, L.M., Ducati, R.G., et al., 2010. Crystal structure and molecular dynamics studies of human purine nucleoside phosphorylase complexed with 7-deazaguanine. J. Struct. Biol. 169, 379-388.

Cole, S.T., Brosch, R., Parkhill, J., Garnier, T., Churcher, C., et al., 1998. Deciphering the biology of *Mycobacterium tuberculosis* from the complete genome sequence. Nature. 393, 537-544.

Collaborative Computational Project Number 4, 1994. The CCP4 suite: programs for protein crystallography. Acta Crystallogr. D Biol. Crystallogr. 50, 760-763.

Darden, T., York, D., Pedersen, L., 1993. Particle mesh Ewald: An N log(N) method for Ewald sums in large systems. J. Chem. Phys. 98, 10089-10092.

de Azevedo Jr., W.F., Canduri, F., dos Santos, D.M., Silva, R.G., de Oliveira, J.S., et al., 2003. Crystal structure of human purine nucleoside phosphorylase at 2.3A resolution. Biochem. Biophys. Res. Commun. 308, 545-552.

Ducati, R.G., Basso, L.A., Santos, D.S., 2007. Mycobacterial shikimate pathway enzymes as targets for drug design. Curr. Drug Targets. 8, 423-435.

Ducati, R.G., Basso, L.A., Santos, D.S., de Azevedo Jr., W.F., 2010a. Crystallographic and docking studies of purine nucleoside phosphorylase from *Mycobacterium tuberculosis*. Bioorg. Med. Chem. 18, 4769-4774.

Ducati, R.G., Breda, A., Basso, L.A., Santos, D.S., 2010b. Purine salvage pathway in *Mycobacterium tuberculosis.* Curr. Med. Chem. 18, 1258-1275.

Ducati, R.G., Ruffino-Netto, A., Basso, L.A., Santos, D.S., 2006. The resumption of consumption - a review on tuberculosis, Mem. Inst. Oswaldo Cruz. 101, 697-714.

Ducati, R.G., Santos, D.S., Basso, L.A., 2009. Substrate specificity and kinetic mechanism of purine nucleoside phosphorylase from *Mycobacterium tuberculosis*. Arch. Biochem. Biophys. 486, 155-164.

Ducati, R.G., Souto, A.A., Caceres, R.A., de Azevedo Jr., W.F., Basso, L.A., et al., 2010c. Purine nucleoside phosphorylase as a molecular target to develop active compounds against *Mycobacterium tuberculosis*. Int. Rev. Biophys. Chem. 1, 34-40.

Friedkin, M., 1950. Desoxyribose-1-phosphate: II. The isolation of crystalline desoxyribose-1-phosphate. J. Biol. Chem. 184, 449-459.

Frisch, M.J., Trucks, G.W., Schlegel, H.B., Scuseria, G.E., Robb, M.A., et al., 2003. Gaussian 03, Gaussian, Wallingford, CT.

Hess, B., 2000. Similarities between principal components of protein dynamics and random diffusion. Phys. Rev. E Stat. Phys. Plasmas Fluids Relat. Interdiscip. Topics, 62 (2000) 8438-8448.

Jackson, M., Berthet, F.X., Otal, I., Rauzier, J., Martin, C., et al., 1996. The *Mycobacterium tuberculosis* purine biosynthetic pathway: isolation and characterization of the *purC* and *purL* genes. Microbiology. 142, 2439-2447.

Kalckar, H.M., 1947. Differential spectrophotometry of purine compounds by means of specific enzymes. 1. Determination of hydroxypurine compounds. J. Biol. Chem. 167, 429-443.

Krissinel, E., Henrick, K., 2007. Inference of macromolecular assemblies from crystalline state. J. Mol. Biol. 372, 774-797.

Laskowski, R.A., MacArthur, M.W., Moss, D.S., Thornton, J.M., 1993. PROCHECK: a program to check the stereochemical quality of protein structures. J. Appl. Cryst. 26, 283-291.

Lewandowicz, A., Shi, W., Evans, G.B., Tyler, P.C., Furneaux, R.H., et al., 2003. Over-the-barrier transition state analogues and crystal structure with *Mycobacterium tuberculosis* purine nucleoside phosphorylase. Biochemistry. 42, 6057-6066.

Mascarenhas, N.M., Bhattacharyya, D., Ghoshal, N., 2010. Why pyridine containing pyrido[2,3-d]pyrimidin-7-ones selectively inhibit CDK4 than CDK2: insights from molecular dynamics simulation. J. Mol. Graph. Model. 28, 695-706.

McRee, D.E., 2004. Differential evolution for protein crystallographic optimizations. Acta Crystallogr. D Biol. Crystallogr. 60, 2276-2279.

Navaza, J., 1994. AMoRe: an automated package for molecular replacement. Acta Crystallogr. A Biol. Crystallogr. 50, 157-16.

Nolasco, D.O., Canduri, F., Pereira, J.H., Cortinóz, J.R., Palma, M.S., et al., 2004. Crystallographic structure of PNP from *Mycobacterium tuberculosis* at 1.9A resolution. Biochem. Biophys. Res. Commun. 324, 789-794.

Nunn, P., Williams, B., Floyd, K., Dye, C., Elzinga, G., et al., 2005. Tuberculosis control in the era of HIV. Nat. Rev. Immunol., 5, 819-826.

O'Brien, R., Haq, I., 2004., Biocalorimetry 2: Applications of Calorimetry in the Biological Sciences, in J.E. Ladbury, M.L. Doyle (Eds.), John Wiley & Sons, Ltd, West Sussex, London, pp.3-34.

Parks Jr., R.E., Agarwal, R.P., 1972. The enzymes, Boyer P.D., ed., Academic Press, New York.

Shi, W., Basso, L.A., Santos, D.S., Tyler, P.C., Furneaux, R.H., et al., 2001. Structures of purine nucleoside phosphorylase from *Mycobacterium tuberculosis* in complexes with immucillin-H and its pieces, Biochemistry. 40, 8204-8215.

Timmers, L.F., Caceres, R.A., Vivan, A.L., Gava, L.M., Dias, R., et al., 2008. Structural studies of human purine nucleoside phosphorylase: towards a new specific empirical scoring function. Arch. Biochem. Biophys. 479, 28-38.

van Aalten, D.M., Bywater, R., Findlay, J.B., Hendlich, M., Hooft, R.W., et al., 1996. PRODRG, a program for generating molecular topologies and unique molecular descriptors from coordinates of small molecules. J. Comput. Aided Mol. Des. 10, 255-262.

van der Spoel, D., Lindahl, E., Hess, B., Groenhof, G., Mark, A.E., et al., 2005. GROMACS: fast, flexible, and free. J. Comput. Chem. 26, 1701-1718.

Villela, A.D., Sánchez-Quitian, Z.A., Ducati, R.G., Santos, D.S., Basso, L.A., 2010. Pyrimidine salvage pathway in *Mycobacterium tuberculosis.* Curr. Med. Chem. 18, 1286-1298.

Figure legends (color)

Fig. 1. Phosphorolysis of inosine catalyzed by MtPNP to ribose 1-phosphate and hypoxanthine.

Fig. 2. Electron density ($2F_{obs}$ - F_{calc}) map contoured at 1σ of INO (A) and HX (B) in the binding-pocket.

Fig. 3. MtPNP:INO:SO_4 and MtPNP:HX schematic drawing. MtPNP is presented as cartoon, and INO, SO_4, and HX as sticks.

Fig. 4. Classical MtPNP binding site. (A) MtPNP:INO:SO_4; (B) MtPNP:HX.

Fig. 5. (A) Radius of gyration between MtPNP:INO:SO_4 (black line) and MtPNP:HX (red line). (B) Root mean square deviation between MtPNP:INO:SO_4 (black line) and MtPNP:HX (red line).

Fig. 6. Total interaction energy between MtPNP:INO:SO_4 and MtPNP:HX. The black line represents the MtPNP:INO:SO_4 interaction energy, and the red line represents the MtPNP:HX interaction energy.

Fig. 7. Displacement of the components of the first eigenvectors for trimeric structures of MtPNP:INO:SO_4 (black line) and MtPNP:HX (red line) complexes. The main fluctuations are presented for regions R1 (Ser36-Phe60), R2 (Ile136-Tyr160),and R3 (Val246-Leu260).

Fig. 8. Isothermal titration calorimetric curves of binding of ligands to MtPNP. (A) Titration of INO substrate. (B) Titration of HX product. The experiments were carried out at constant temperature and pressure.

Table legends

Table 1. Data collection and refinement statistics. Values in parentheses refer to the highest resolution shell.

Table 2. Eigenvalues (EV) and cumulative eigenvalues (CV) of the covariance matrix resulting from MtPNP:INO:SO_4 and MtPNP:HX simulations.

Figure 1

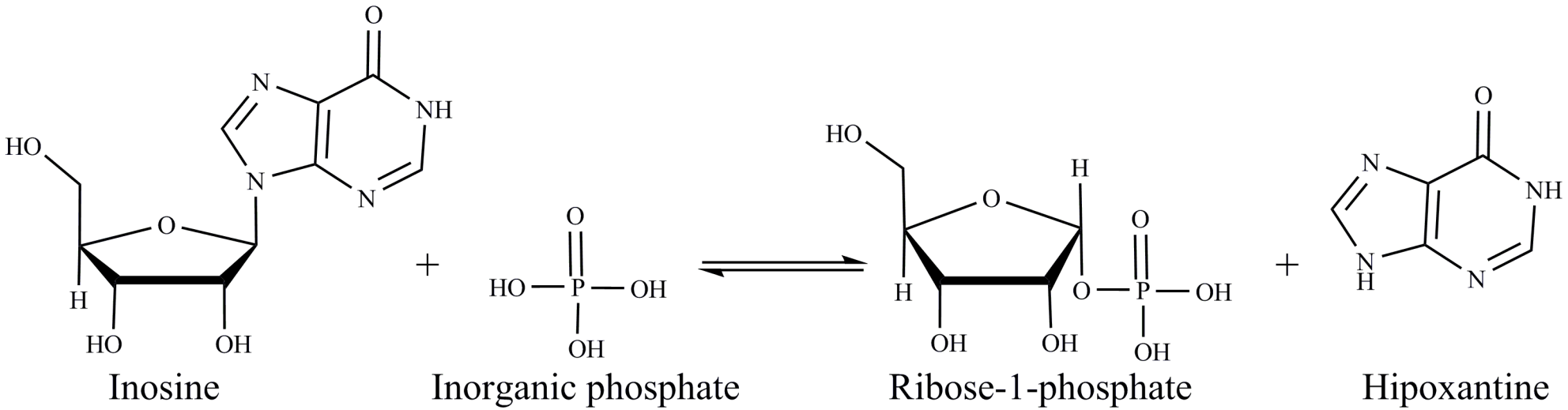
Inosine
Inorganic phosphate
Ribose-1-phosphate
Hipoxantine

Figure 2

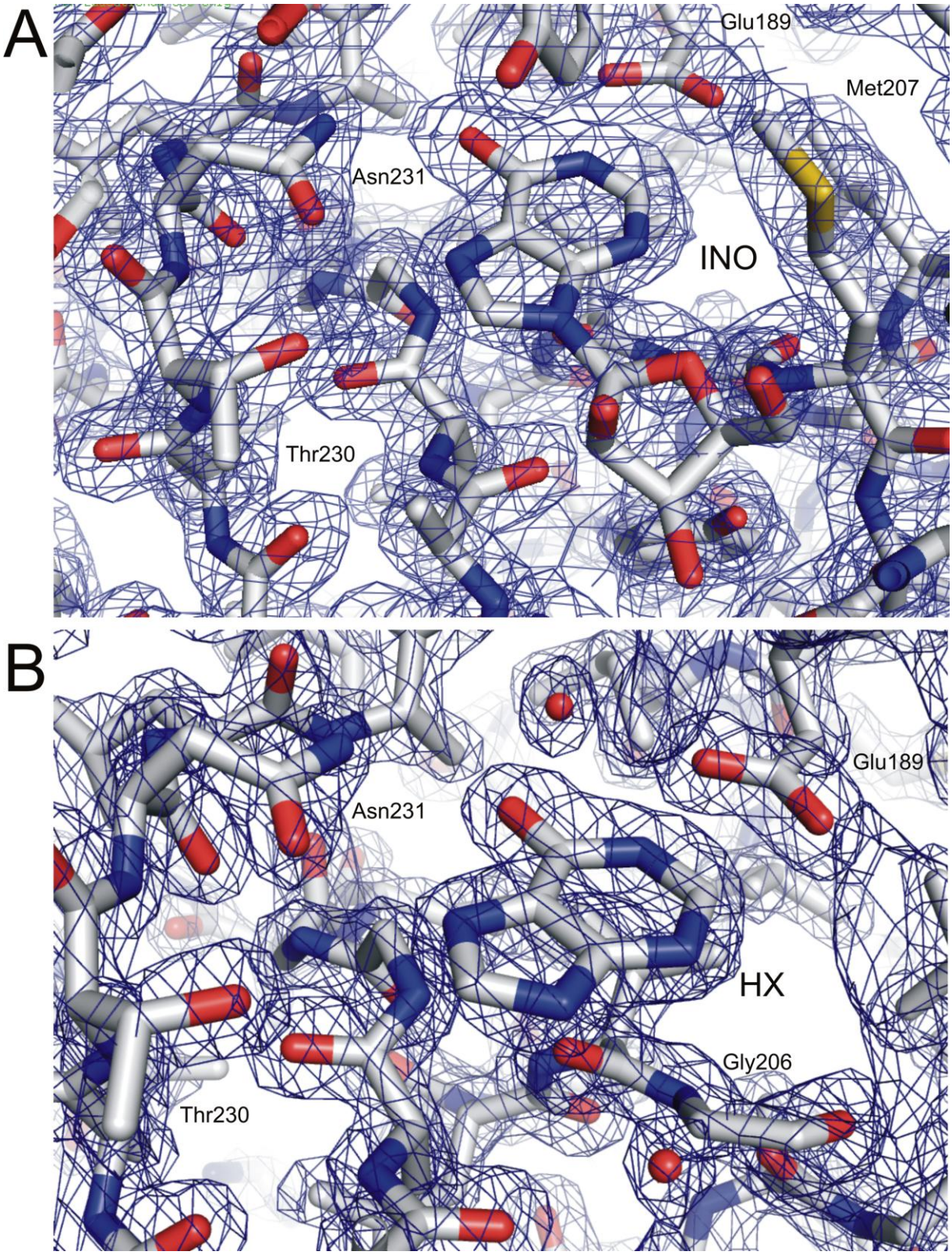
A
Glu189
Met207
Asn231
INO
Thr230
B
Asn231
Glu189
HX
Gly206
Thr230

Figure 3

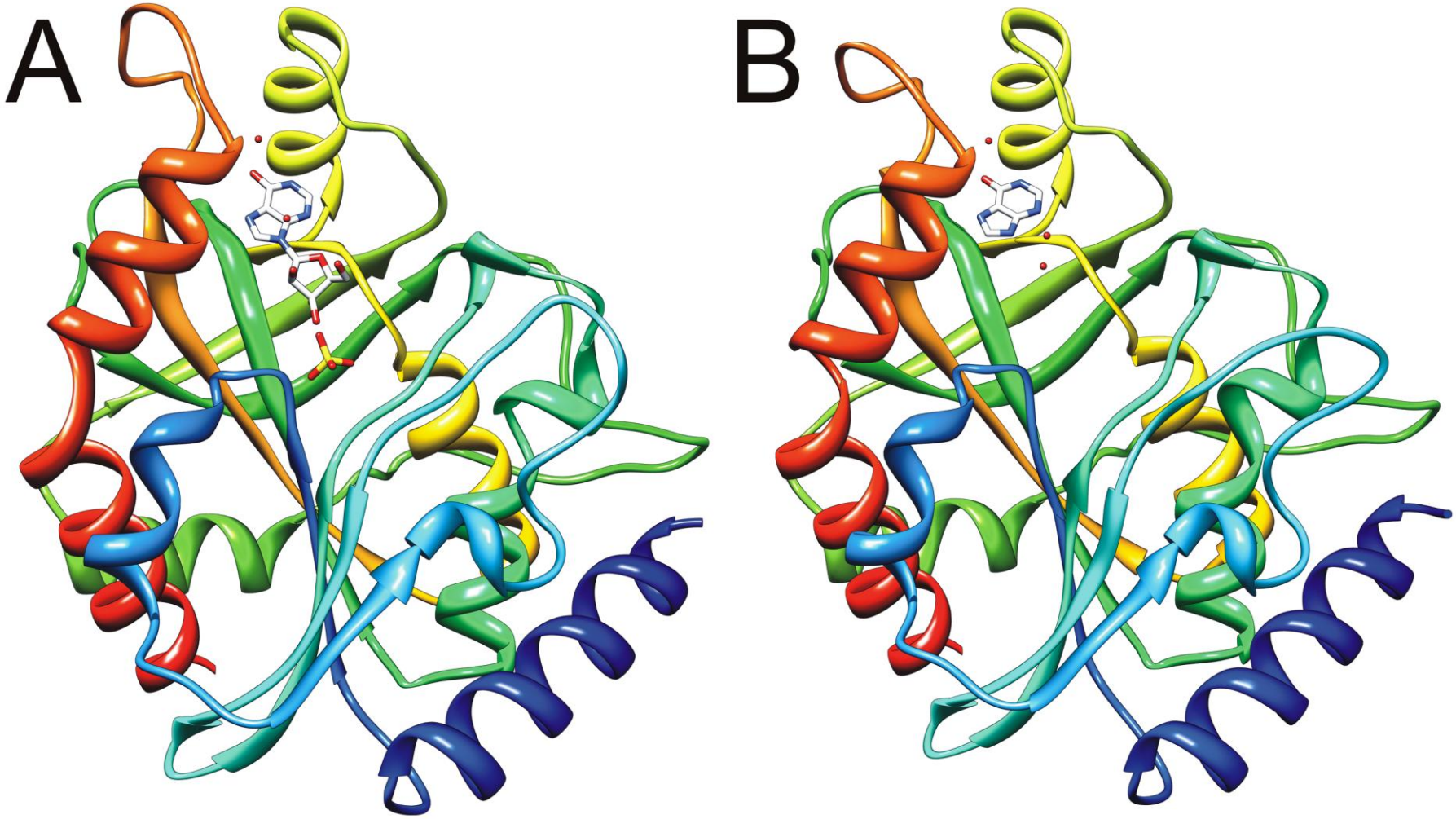

Figure 4

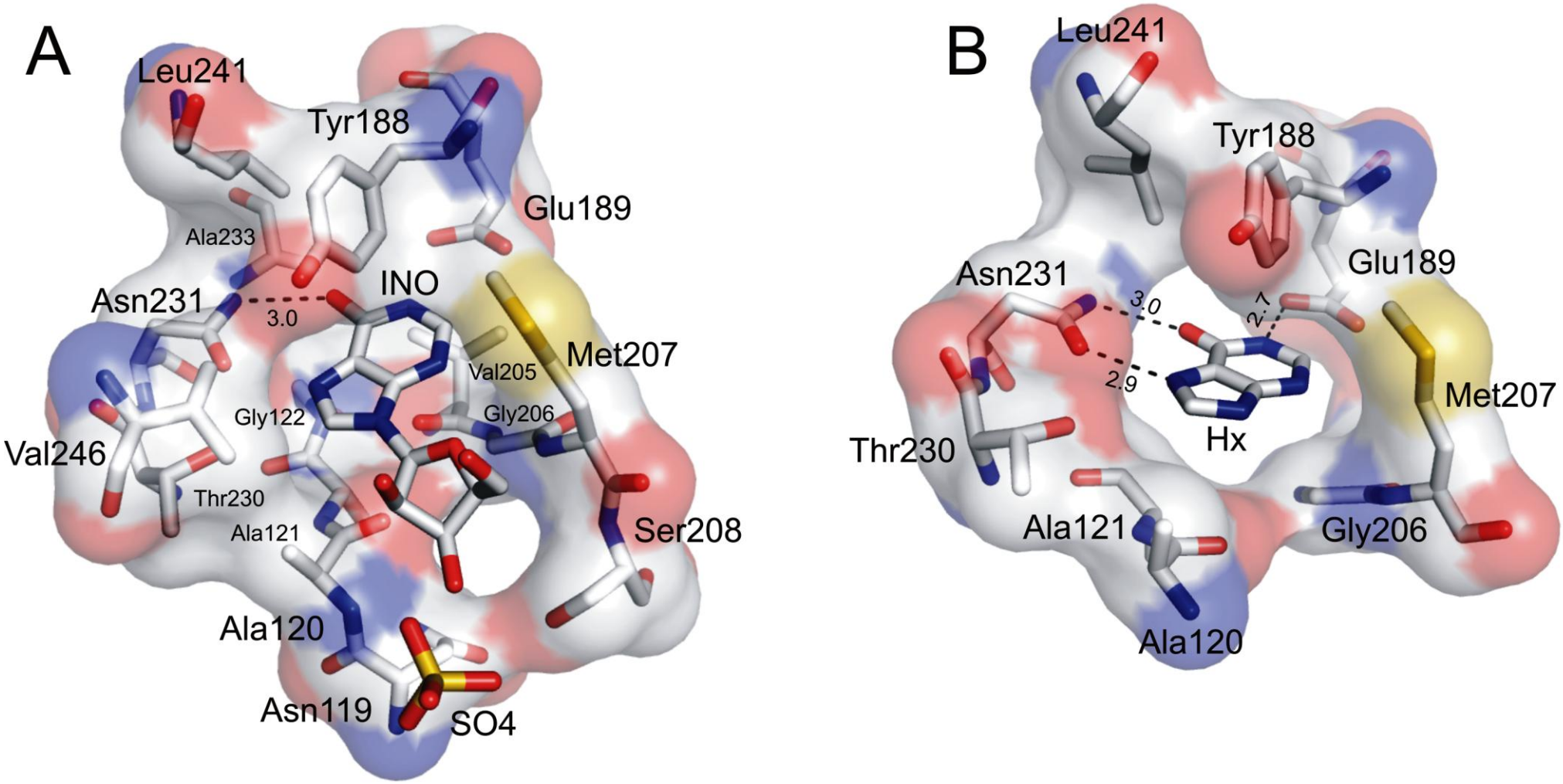
A
Leu241
Tyr188
Glu189
Ala233
INO
Asn231
3.0
Met207
Val205
Gly122
Gly206
Val246
Thr230
Ala121
Ser208
Ala120
Asn119
SO4
B
Leu241
Tyr188
Glu189
Asn231
3.0
2.9
Met207
Hx
Thr230
Ala121
Gly206
Ala120

Figure 5

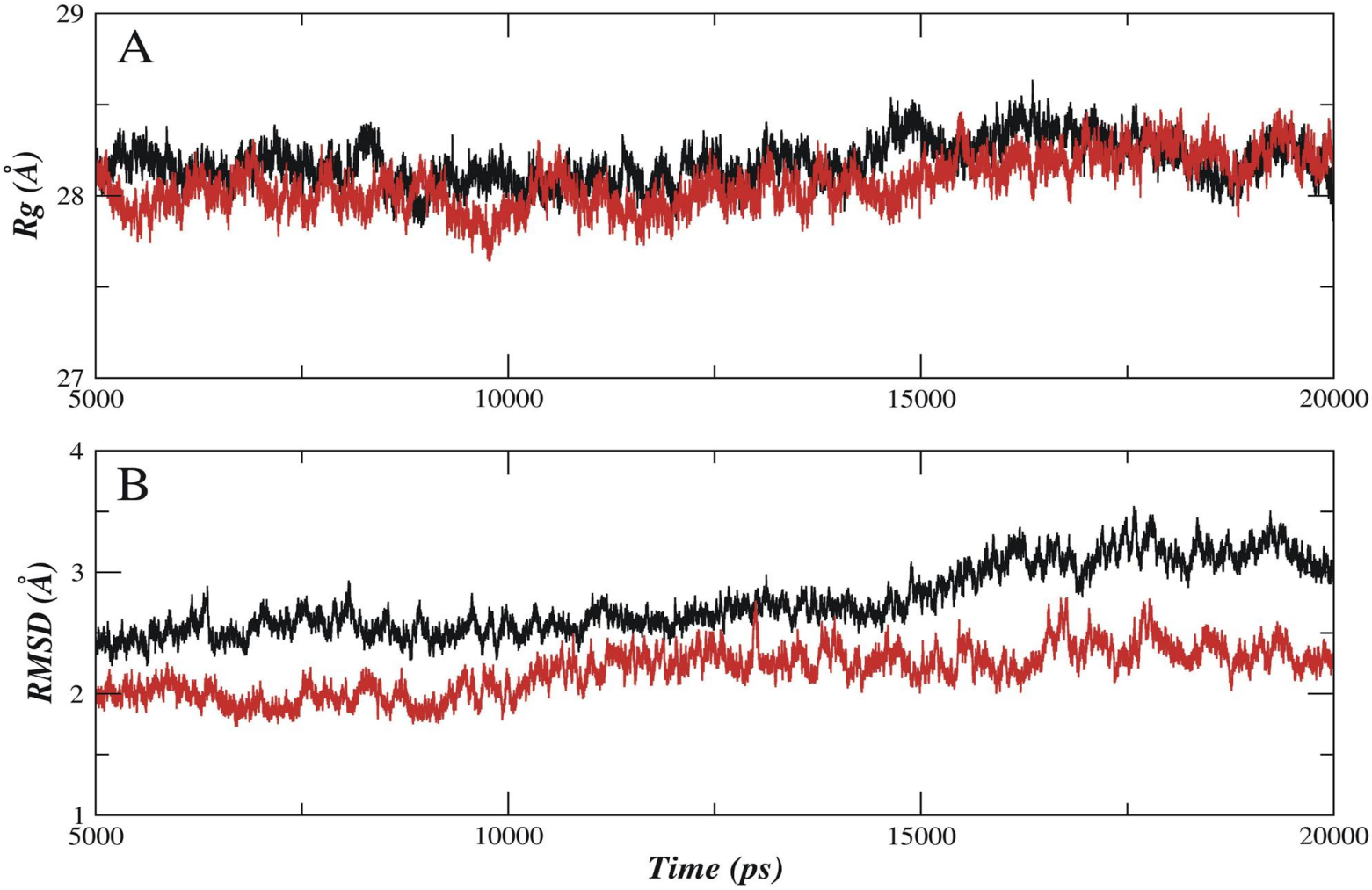

Figure 6

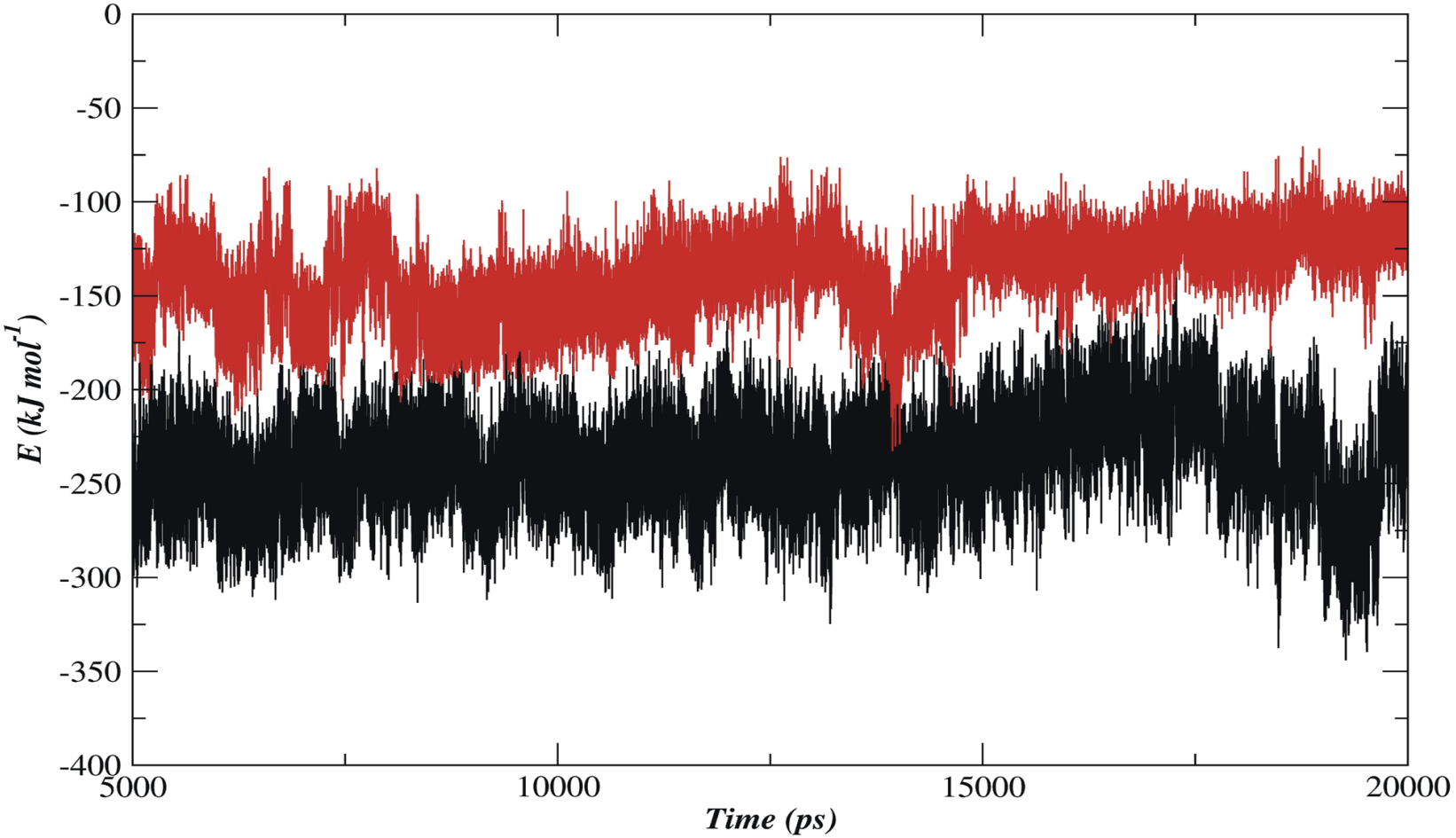
0
-50
-100
-150
-200
-250
-300
-350
-400
5000
10000
15000
20000
E (kJ mol-1)
Time (ps)

Figure 7

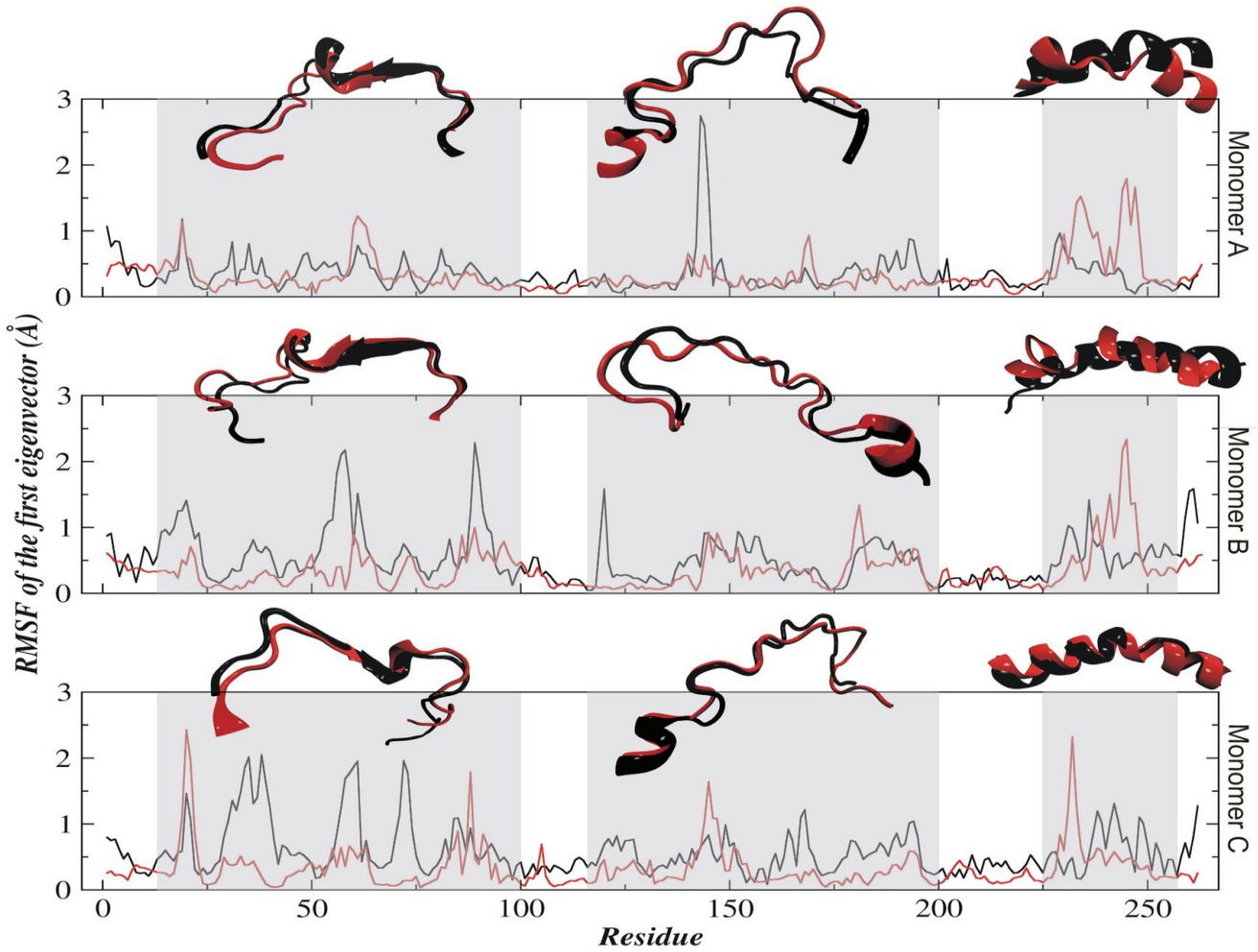
RMSF of the first eigenvector (Å)
Residue
Monomer A
Monomer B
Monomer C
0
1
2
3
0
50
100
150
200
250

Figure 8

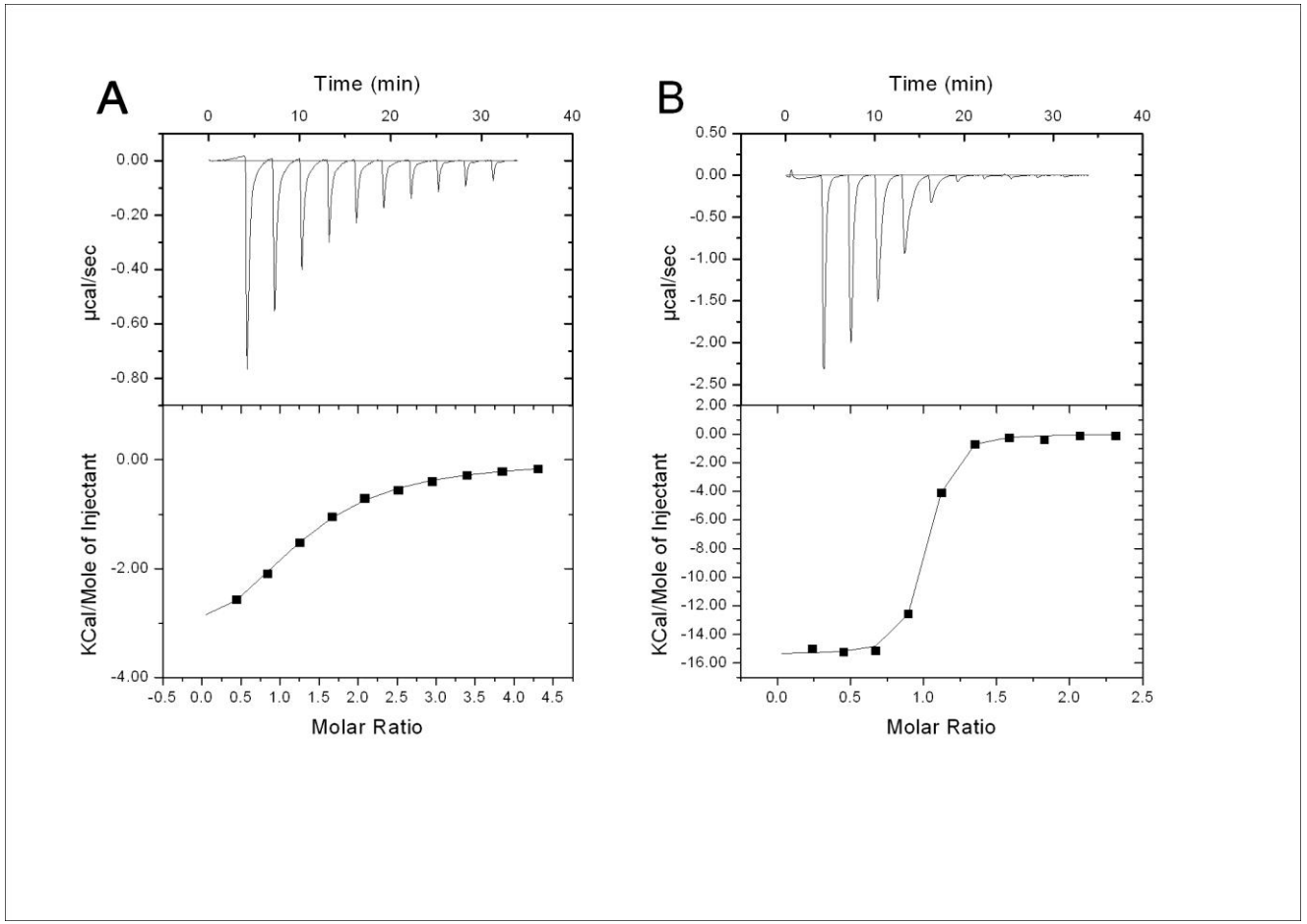
A
Time (min)
0
10
20
30
40
0.00
-0.20
-0.40
-0.60
-0.80
µcal/sec
0.00
-2.00
-4.00
KCal/Mole of Injectant
-0.5
0.0
0.5
1.0
1.5
2.0
2.5
3.0
3.5
4.0
4.5
Molar Ratio
B
Time (min)
0
10
20
30
40
0.50
0.00
-0.50
-1.00
-1.50
-2.00
-2.50
µcal/sec
2.00
0.00
-2.00
-4.00
-6.00
-8.00
-10.00
-12.00
-14.00
-16.00
KCal/Mole of Injectant
0.0
0.5
1.0
1.5
2.0
2.5
Molar Ratio

Table 1

Data collection and refinement statistics*	MtPNP:INO:SO4	MtPNP:HX
X-ray wavelength (Å)	1.427	1.427
Temperature (K)	100	100
Resolution range (Å)	28.55 (1.99)	21.09 (1.95)
Space group	H3	H3
Unit-cell parameters		
a = b (Å)	115.80	115.59
c (Å)	86.77	86.30
α = β (º)	90.00	90.00
γ (º)	120	120
Highest Resolution Shell (Å)	1.99	1.95
Data completeness (%)	98.73	100
R_{merge} (%) [a]	6.1	7.4
Resolution range used in refinement (Å)	2.03 - 1.99	2.00 - 1.95
R_{factor} (%) [b]	18.04	17.37
R_{free} (%) [c]	23.53	22.77
Observed RMSD from the ideal geometry		
Bond lenghts (Å)	0.020	0.018
Bond angles (º)	1.856	1.611
B values (Å)^2 [d]	18.896	17.221
Residues in most favored regions of the Ramachandran plot (%)	90.7	91.2
Residues in additionally allowed regions of the Ramachandran plot (%)	8.1	7.9
Residues in generously allowed regions of the Ramachandran plot (%)	0.7	0.5
Residues in disallowed regions of the Ramachandran plot (%)	0.5	0.5
Number of ligands	2	2
Number of water molecules	269	280

[a] $R_{merge} = \Sigma_h \Sigma_i |I(h)_i - \langle I(h) \rangle| / \Sigma_h \Sigma_i I(h)_i$, where I(*h*) is the intensity of reflection *h*, $\sum_h$ is the sum over all reflections and Σ_i is the sum over *i* measurements

[b] $R_{factor} = 100 \times \Sigma|F_{obs} - F_{calc}| / \Sigma(F_{obs})$, the sums being taken over all reflections with $F / \sigma(F) > 2$ cutoff.

[c] $R_{free} = R_{factor}$ for 10% of the data, which were not included during crystallographic refinement.

[d] B values = average B values for all non-hydrogen atoms.

* Values in parenthesis refer to the highest resolution shell

Table 2

Structure		Monomer A		Monomer B		Monomer C		Structure		Monomer A		Monomer B		Monomer C	
	Eigenvector	EV[a]	CV[b]	EV	CV	EV	CV		Eigenvector	EV	CV	EV	CV	EV	CV
$MtPNP:INO:SO_4$	1	53.69	20.35	112.79	33.73	126.49	38.93	MtPNP:HX	1	50.98	19.76	59.01	22.75	55.83	24.25
	2	26.35	30.33	25.20	41.27	25.05	46.64		2	27.25	30.32	34.30	35.98	17.37	31.80
	3	21.85	38.61	24.22	48.51	16.92	51.85		3	13.52	35.56	14.79	41.68	10.35	36.30
	4	15.08	44.33	12.05	52.11	13.89	56.12		4	11.42	39.99	10.35	45.67	8.85	40.14
	5	9.41	47.90	11.00	55.40	10.15	59.25		5	10.30	43.98	8.64	49.00	8.36	43.77
	6	9.00	51.31	10.84	58.65	7.48	61.55		6	9.44	47.64	8.15	52.14	6.73	46.69
	7	5.76	53.69	8.90	61.31	6.48	63.54		7	7.43	50.52	6.12	54.50	6.07	49.33
	8	5.36	55.88	6.49	63.25	5.59	65.27		8	6.05	52.86	5.63	56.68	4.80	51.42
	9	4.32	57.91	5.95	65.03	4.85	66.76		9	5.26	54.90	4.77	58.51	4.69	53.45
	10	4.07	59.55	5.13	66.56	4.49	68.14		10	4.36	56.59	3.57	59.89	4.24	55.29

[a] Eigenvalues of covariance matrix (A^2)

[b] Cumulative sum values (%)

Capítulo 8

Considerações finais

8 Considerações finais

A resolução das estruturas dos complexos MtPNP:Ino:SO_4, MtPNP:Hx e MtPNP:Acy:PO_4 fornecem preciosas informações estruturais, principalmente sobre o sítio ativo da PNP em associação com produtos, substratos e inibidores. Com essas informações adicionais, iniciativas de desenvolvimento de fármacos baseados na estrutura poderão ser favorecidas já que estruturas resolvidas destes complexos são escassas. Nestes complexos podemos observar que os principais resíduos que interagem com os ligantes, através de ligações de hidrogênio, são o Glu189 e a Asn231, ancorando-os no sítio ativo. Estes resíduos frequentemente participam no processo de interação de ligantes, e, portanto, devem ser levados em consideração no desenvolvimento de possíveis inibidores de PNP.

Apesar da cristalografia de macromoléculas biológicas ser uma técnica poderosa na determinação de estrutura 3D de proteína e seus complexos, ela apresenta algumas limitações, destacando-se a incapacidade de se analisar o comportamento dinâmico destas macromoléculas em solução. Para contornar esta limitação a DM foi utilizada com sucesso, fornecendo informações inéditas. Aliado à DM, a utilização da análise por PCA ou *essential dynamics* (ED) nas simulações forneceu uma sofisticação metodológica permitindo uma maior clareza dos resultados, já que a redução da complexidade dos dados e a investigação dos movimentos mais significativos durante a simulação fornecem um panorama mais realista da simulação.

Por meio das simulações de DM dos complexos resolvidos pode-se observar que a Phe153 de MtPNP, se comparada com a Phe159 da PNP de humanos,

(HsPNP) não parece desempenhar o mesmo papel. Enquanto que a Phe153 da MtPNP esta implicada na manutenção da estrutura quaternária da enzima a Phe159 na HsPNP exerce um papel fundamental na especificidade do ligante, pois quando o sítio de purina do monômero adjacente é ocupado a Phe159 aproxima-se deste sítio revelando um mecanismo do tipo tampa (LID), o que não ocorre na Phe153 evidenciado pelo flutuação média quadrática do primeiro autovetor (RMSF) e do B-factor não se alterarem nas simulações com e sem a presença dos ligantes (Hx, Ino e ACY).

O *web server* chamado SEA (similarity ensemble approach) demonstrou ser uma ferramenta valiosa na verificação de possível atividade inibidora contra alvos moleculares, como já havia demonstrado em outro estudo (Keiser *et al*., 2009), em que se verificou a capacidade de drogas disponíveis no mercado em ligar-se em diversos alvos moleculares, característica que pode ser demonstrada nos efeitos colaterais causados pela ação deste fármaco.. O SEA forneceu um valor E de 1,12 x 10^{-122} e um coeficiente de Tanimoto de 56 %, estes resultados inferem que o ACY poderia ser um inibidor frente a MtPNP. Este resultado se deve provavelmente pela similaridade da fração purínica entre o ACY e o Imucilim, um conhecido e potente inibidor de PNP.

O ITC (Isothermal Titration Calorimetry) é uma importante ferramenta para a descoberta de novos compostos líderes, graças a sua capacidade em um único experimento, determinar a afinidade e o perfil termodinâmico, que auxilia na compreensão das mudanças comformacionais quando da formação dos complexos binários. Os valores de ITC indicaram uma preferência da MtPNP pela Hx, isto indica que termodinamicamente o equilíbrio da reação é deslocado no sentido da síntese de nucleosídeos. No entanto, *in vivo*, a fosforólise é altamente favorecida em relação à síntese devido ao

acoplamento de duas reações enzimáticas, a oxidação seguida da fosforilação seguida pela liberação da base púrica pela xantina oxidase e hipoxantina fosforribosil-transferase, respectivamente.

A aplicação de diferentes abordagens, bem como a união das técnicas de bioinformática com técnicas experimentais, para o melhor entendimento do problema biológico, é um dos fatores que devem ser ressaltados neste trabalho.

Além disso, os dados fornecidos pelas estruturas dos complexos resolvidos são essenciais, uma vez que informações de inibidores de MtPNP são extremamente escassos e são fundamentais em modelos de QSAR (Quantitative Structure-Activity Relationship - relação estrutura e atividade quantitativa) bem como no desenvolvimento de funções *scores* específicas.

Referências

Referências

Allen MP, Tildesley DJ. *Computer Simulation of Liquids*. Oxford University Press. 1987

Amadei A, Linssen AB, Berendsen HJ. Essential dynamics of proteins. Proteins 1993; 17(4):412-425.

Basso LA, Zheng R, Musser JM, Jacobs WR Jr, Blanchard JS. Mechanisms of isoniazid resistance in Mycobacterium tuberculosis: Enzymatic characterization of enoyl reductase mutants identified in isoniazid-resistant clinical isolates. J. Infect. Dis. 1998; 178(3):769-775.

Basso LA, Santos DS, Shi W, Furneaux RH, Tyler PC, Schramm VL, Blanchard JS. Purine nucleoside phosphorylase from Mycobacterium tuberculosis. Analysis of inhibition by a transition-state analogue and dissection by parts. Biochemistry 2001; 40(28):8196-8203.

Baptista IMFD, Oelemann MC, Opromolla DV, Suffys PN. Drug Resistance and Genotypes of Strains of *Mycobacterium tuberculosis* Isolated from Human Immunodeficiency Virus-infected and Non-infected Tuberculosis Patients in Bauru, São Paulo, Brazil. Mem. Inst. Owaldo Cruz 2002; 97(8): 1147-1152.

Berman HM, Battistuz T, Bhat TN, Bluhm WF, Bourne PE, Burkhardt K, Iype L, Jain S, Fagan P, Marvin J, Padilla D, Ravichandran V, Schneider B, Thanki N, Weissig H, Westbrook JD, Zardecki C. The Protein Data Bank. Acta Crystallogr. D Biol. Crystallogr. 2002; 58(1): 899-907.

Bloom BR, Murray CJL. Tuberculosis - Commentary on a Reemergent Killer. Science 1992; 257(5073): 1055-1064.

Blundell TL, Johnson, LN. Protein Crystallography. London: Academic Press. 1976.

Bzowska A, Kulikowska E, Shugar D. Purine nucleoside phosphorylases: properties, functions, and clinical aspects. Pharmacol. & Ther. 2000; 88(3): 349-425.

Canduri F, dos Santos DM, Silva RG, Mendes MA, Basso LA, Palma MS, de Azevedo WF, Santos DS. Structures of human purine nucleoside phosphorylase complexed with inosine and ddI. Biochem. Biophys. Res. Commun. 2004; 313(4): 907-914.

Clemmens DL. Characterization of the Mycobacterium tuberculosis phagosome. Trends Mycrobiol. 1996; 4(3): 113-118.

Corbett EL, Watt CJ, Walker N, Mahier D, Williams BG, Raviglione MC, Dye C. The growing burden of tuberculosis - Global trends and interactions with the HIV epidemic. Arch. Intern. Med. 2003; 163(9): 1009-1021.

De Azevedo WF Jr., Canduri F, dos Santos DM, Silva RG, de Oliveira JS, de Carvalho LP, Basso LA, Mendes MA, Palma MS, Santos DS. Crystal structure of human purine nucleoside phosphorylase at 2.3 angstrom resolution. Biochem. Biophys. Res. Commun. 2003; 308(3): 545-552.

Drobniewski FA, Caws M, Gibson A, Young D. Modern laboratory diagnosis of tuberculosis. The Lancet Infect. Dis. 2003; 3(3): 141-147.

Ducati RG, Santos DS, Basso LA. Substrate specificity and kinetic mechanism of purine nucleoside phosphorylase from Mycobacterium tuberculosis. Arch. Biochem. Biophys. 2009; 486(2): 155-164.

Ducati RG, Basso LA, Santos DS, de Azevedo WF Jr. Crystallographic and docking studies of purine nucleoside phosphorylase from Mycobacterium tuberculosis. Bioorg. & Med. Chem. 2010; 18(13): 4769-4774.

Ducruix A, Giegé R. Crystallization of nucleic acids and proteins. A practical approach. Oxford, UK: IRL Press. 1992.

Duncan K. Progress in TB drug development and what is still needed. Tuberculosis 2003; 83(1-3): 201-207.

el Kouni MH. Potential chemotherapeutic targets in the purine metabolism of parasites Pharmacol. Ther. 2003; 99(3): 283-309.

El Sayed K, Bartyzel P, Shen XY, Perry TL, Kjawiony JK, Hamann MT. Marine natural products as antituberculosis agents. Tetrahedron 2000; 56(7): 949-953.

Funasa, 2002. Situação da Prevenção e Controle de Doenças Transmissíveis no Brasil. Setembro/2002 [http://www.funasa.gov.br/guia_epi/]

Guex N, Peitsch MC. SWISS-MODEL and the Swiss-PdbViewer: An environment for comparative protein modeling. Electrophoresis. 1997; 18(15): 2714-2723.

Hayward S, Kitao A, Go N. Harmonic and anharmonic aspects in the dynamics of BPTI: A normal mode analysis and principal component analysis. Protein Sci. 1994; 3(6): 936-943.

Hiriyanna KT, Ramakrishnam,T. Deoxyribonucleic-acid replication time in mycobacterium-tuberculosis H37Rv. Mycobacterium tuberculosis Arch. Microbiol. 1986; 144(2): 105-109.

Jensen KF, Nygaard P. Purine Nucleoside Phosphorylase from Escherichia-coli and Salmonella-typhimurium - Purification and Some Properties. Eur. J. Biochem. 1975; 51(1): 253-265.

Keiser MJ, Setola V, Irwin JJ, Laggner C, Abbas AI, Hufeisen SJ, Jensen NH, Kuijer MB, Matos RC, Tran TB, Whaley R, Glennon RA, Hert J, Thomas KLH, Edwards DD, Shoichet BK, Roth BL. Predictind New Molecular Targets for Known Drugs. Nature 2009; 462(12):175-182.

Manabe YC, Bishai WR. Latent Mycobacterium tuberculosis - persistence, patience, and winning by waiting. Nat. Med. 2000; 6(12): 1327-1329.

Marion JB, Thornton ST. Classical Dynamics of Particles and Systems 4ª Ed., Saunders College Publishing. 1995.

Mascarenhas, N.M., Bhattacharyya, D., Ghoshal, N. (2010) J. Mol. Graph. Model. 28, 695-706.

Parker WB, Long MC. Purine metabolism in Mycobacterium tuberculosis as a target for drug development. Curr. Pharm. Des. 2007; 13(6): 599-608.

Pivetta M. Ferro na tuberculose. Pesquisa Fapesp 2004; 97(3): 32-37.

Shi W, Basso LA, Santos DS, Tyler PC, Furneaux RH, Blanchard JS, Almo SC, Schramm VL. Structures of purine nucleoside phosphorylase from Mycobacterium tuberculosis in complexes with immucillin-H and its pieces. Biochemistry 2001; 40(28): 8204-8215.

Stoeckler JD, Poirot AF, Smith RM, Parks RE Jr, Ealick SE, Takabayashi K, Erion MD. Purine Nucleoside Phosphorylase. 3. Reversal of Purine Base Specificity by Site-Directed Mutagenesis. Biochemistry 1997; 36(39): 11749-11756.

Tozzi M, Camici M, Mascia L, Sgarrella F, Ipata P. Pentose phosphates in nucleoside interconvertion and catabolism. FEBS J. 2010; (6): 1089-1101.

Trouiller P, Torreele E, Olliaro P, White N, Foster S, Wirth D, Pecoul B. Drugs for neglected diseases: a failure of the market and a public health failure? Trop. Med. Int. Health. 2001; 6(11): 945-951.

van Gunsteren WF, Berendsen HJC. Computer-Simulation of Molecular-Dynamics - Methodology, Applications, and Perspectives in Chemistry. Angewandte Chemie-International Edition in English. 1990; 29(9):992 -1023.

Velayati AA, Farnia P, Masjedi MR, Ibrahim TA, Tabarsi P, Haroun RZ, Kuan HO, Ghanavi P, Farnia P, Varahram M. Totally drug-resistant tuberculosis strains: evidence of adaptation at the cellular level. Eur. Respir. J. 2009; 34(5): 1202-1203

Verlet L. Computer "Experiments" on Classical Fluids. II. Equilibrium Correlation Functions. Phys. Rev. 1968; 165(1): 201-214.

WHO, 2001. Stop TB Annual report 2001. World Health Organization, Geneva, Switzerland, WHO/CDS/STB/2002.17

WHO, 2002. Tuberculosis Fact Sheet Nº 104. World Health Organization, Geneva, Switzerland.August/2002

WHO, 2003. The global plan to stop tuberculosis. World Health Organization, Geneva, Switzerland, WHO/CDS/STB/2003.23

World Health Organization. WHO Report, 2004. Geneva. Switzerland. WHO/CDS/TB/2004.331.

WHO, 2004a. Tuberculosis. Fact Sheet Nº 104. World Health Organization, Geneva, Switzerland.March2004

WHO, 2004b. Global tuberculosis control. In WHO Report 2004. World Health Geneva, Switzerland, WHO/HTM/TB/2004.331

WHO, 2009. Global tuberculosis control: a short update to the 2009 report. World Health Geneva, Switzerland. December/2009.

Zimmerman TP, Gersten NB, Ross AF, Miech RP. Adenine as Substrate for Purine Nucleoside Phosphorylase. Can. J Biochem. 1971; 49(9): 1050-1054.

Anexos

A. Carta de aceite do artigo Purine Nucleoside Phosphorylase as a Molecular Target to Develop Active Compounds Against *Mycobacterium tuberculosis* publicado no IREBIC

B. Carta de aceite do artigo Crystal structure and molecular dynamics studies of purine nucleoside phosphorylase from *Mycobacterium tuberculosis* associated with acyclovir publicado na BIOCHIMIE

C. Carta de submissão ao JMB

D. Artigos publicados no período

Anexo A

Carta de aceite do artigo Purine Nucleoside Phosphorylase as a Molecular Target to Develop Active Compounds Against *Mycobacterium tuberculosis* publicado no International Review of Biophysical Chemistry

From: Praise Worthy Prize [mailto:info@praiseworthyprize.it]
Sent: Tue 9/7/2010 6:38 AM
To: Luiz Augusto Basso
Subject: Purine Nucleoside Phosphorylase as a Molecular Target to Develop Active Compounds Against Mycobacterium tuberculosis

Dear Prof. Basso

It is my great pleasure to inform you that your paper (ID 3654) has been accepted and will be published on the ***International Review of Biophysical Chemistry (IREBIC).***
Congratulations!

If you want to publish the paper on the August issue of the Review, please, accomplish the following requirements as soon as possible.

The prerequisites in order to publish your paper, are the following:

1. **you should change the paper according to the following remarks of the reviewers:**

Both the name and structure of one compound in Fig. 5 are erroneously reported. SA-ImmH should be SA-ImmG, as it is a deazaguanine derivative. Accordingly, its structure presents a NH2 group at position 2 (like BCX-34). Moreover, in the side chain at position 9 every OH group is connected to nitrogen by a two-methylene chain.
Also in the text, please correct SA-ImmH into SA-ImmG.

2- you should complete, sign and return, by fax, to the number +39 0810360768 the following documents (SEE THE ENCLOSED FILES)**:**

1. **copy of the COPYRIGHT FORM;**
2. **copy of the TREATMENT OF PERSONAL DATA.**
3. **eventually a copy of the PERMISSION REQUEST FORM for the reproduction of any figure, table or extensive (more than fifty words) extract from the text of a source that is copyrighted or owned by a party other than Praise Worthy Prize or of the Author.**

Best Regards

Anna Bosso
Head of the Editorial Staff
Best Regards

Anna Bosso
Head of the Editorial Staff

****

PRAISE WORTHY PRIZE S.r.l.
PUBLISHING HOUSE
Editorial Staff

editorialstaff@praiseworthyprize.com

++++++++++++++++++++++ ATTENTION
++

Anexo B

Carta de aceite do artigo Crystal structure and molecular dynamics studies of purine nucleoside phosphorylase from *Mycobacterium tuberculosis* associated with acyclovir
publicado na Biochimie

Date: 11/10/2011 To: "Walter Filgueira de Azevedo Jr." walter@azevedolab.net
From: "Biochimie" Redaction.Biochimie@ibpc.fr Subject: Your Submission

Ref.: Ms. No. BIOCHI-D-11-00280R1
Crystal structure and molecular dynamics studies of purine nucleoside phosphorylase from Mycobacterium tuberculosis associated with acyclovir
Biochimie

Dear Dr. Filgueira de Azevedo,

I am pleased to tell you that your work has now been accepted for publication in Biochimie.

Thank you for submitting your work to this journal.

For further assistance, please visit our customer support site at http://support.elsevier.com. Here you can search for solutions on a range of topics, find answers to frequently asked questions and learn more about EES via interactive tutorials. You will also find our 24/7 support contact details should you need any further assistance from one of our customer support representatives.

With kind regards

Richard H. Buckingham
Regional Editor
Biochimie

Anexo C

Artigos publicados no período de doutoramento (2008-2011)

1. SANCHEZ-QUITIAN, Z.A., TIMMERS, L.F.S.M., **CACERES, R.A.**, REHM, J.G., THOMPSON, C.E., BASSO, L.A., DE AZEVEDO, W.F., SANTOS, D.S. Crystal structure determination and dynamic studies of Mycobacterium tuberculosis Cytidine deaminase in complex with products. Archives of Biochemistry and Biophysics (Print). , v.509, p.108 - 115, 2011.

2. **CACERES, R.A.**, TIMMERS, L.F.S.M., PAULI, I., GAVA, L.M., DUCATI, R. G., BASSO, L.A., SANTOS, D.S., DE AZEVEDO, W.F. Crystal structure and molecular dynamics studies of human purine nucleoside phosphorylase complexed with 7-deazaguanine. Journal of Structural Biology. , v.169, p.379 - 388, 2010.

3. **CACERES, R.A.**, ZANCHI, F.B., STABELI, R.G., DE AZEVEDO, W.F. Molecular dynamics studies of a hexameric purine nucleoside phosphorylase. Journal of Molecular Modeling. , v.16, p.543 - 550, 2010.

4. DUCATI, R.G., SOUTO, A.A., **CACERES, R.A.**, DE AZEVEDO, W.F., BASSO, L.A., SANTOS, D.S. Purine Nucleoside Phosphorylase as a Molecular Target to Develop Active Compounds Against Mycobacterium tuberculosis. International Review of Biophysical Chemistry - IREBIC. , v.1, p.34 - 40, 2010.

5. DE AZEVEDO, W.F., DIAS, R., TIMMERS, L.F.S.M., PAULI, I., **CACERES, R.A.**, SOARES, M.B.P. Bioinformatics Tools for Screening of Antiparasitic Drugs. Current Drug Targets. , v.10, p.232 - 239, 2009.

6. TIMMERS, L.F.S.M., PAULI, I., BARCELLOS, G.B., ROCHA, K.B., **CACERES, R.A.**, DE AZEVEDO, W.F., SOARES, M.B.P. Genomic Databases and the Search of Protein Targets for Protozoan Parasites. Current Drug Targets. , v.10, p.240 - 245, 2009.

7. PEREZ, P.C., **CACERES, R.A.**, CANDURI, F., DE AZEVEDO, W.F. Molecular modeling and dynamics simulation of human cyclin-dependent kinase 3 complexed with inhibtors. Computers in Biology and Medicine. , v.39, p.130 - 140, 2009.

8. PAULI, I., TIMMERS, L.F.S.M., **CACERES, R.A.**, BASSO, L.A., SANTOS, D.S., DE AZEVEDO, W.F. Molecular modeling and dynamics studies of purine nucleoside phosphorylase from Bacteroides fragilis. Journal of Molecular Modeling. , v.15, p.913 - 922, 2009.

9. TIMMERS, L.F.S.M., **CACERES, R.A.**, DIAS, R., BASSO, L.A., SANTOS, D.S., DE AZEVEDO, W.F. Molecular modeling, dynamics and docking studies of Purine Nucleoside Phosphorylase. Biophysical Chemistry (Print). , v.142, p.7 - 16, 2009.

10. DE AZEVEDO, W.F., **CACERES, R.A.**, PAULI, I., TIMMERS, L.F.S.M., BARCELLOS, G.B., ROCHA, K.B., SOARES, M.B.P. Protein-Drug Interaction Studies for Development of Drugs Against Plasmodium falciparum. Current Drug Targets. , v.10, p.271 - 278, 2009.

11. VIVAN, A.L., **CACERES, R.A.**, BASSO, L.A., SANTOS, D.S., DE AZEVEDO, W.F. Structural studies of PNP from Toxoplasma gondii. International Journal of Bioinformatics Research and Applications (Print). , v.5, p.154 - 162, 2009.

12. BARCELLOS, G.B., **CACERES, R.A.**, DE AZEVEDO, W.F. Structural studies of shikimate dehydrogenase from Bacillus anthracis complexed with cofactor NADP. Journal of Molecular Modeling. , v.15, p.147 - 155, 2009.

13. CANDURI, F., PEREZ, P.C., **CACERES, R.A.**, DE AZEVEDO, W.F. CDK9 a Potential Target for Drug Development. Medicinal Chemistry. , v.4, p.210 - 218, 2008.

14. TIMMERS, L.F.S.M., PAULI, I., **CACERES, R.A.**, DE AZEVEDO, W.F. Drug-Binding Databases. Current Drug Targets. , v.9, p.1092 - 1099, 2008.

15. DIAS, R., TIMMERS, L.F.S.M., **CACERES, R.A.**, DE AZEVEDO, W.F. Evaluation of Molecular Docking Using Polynomial Empirical Scoring Functions. Current Drug Targets. , v.9, p.1062 - 1070, 2008.

16. PAULI, I., TIMMERS, L.F.S.M., **CACERES, R.A.**, SOARES, M.B.P., DE AZEVEDO, W.F. In Silico and In Vitro: Identifying New Drugs. Current Drug Targets. , v.9, p.1054 - 1061, 2008.

17. AMORIM, H.L.N., **CACERES, R.A.**, NETZ, P. A. Linear Interaction Energy (LIE) Method in Lead Discovery and Optimization. Current Drug Targets. , v.9, p.1100 - 1105, 2008.

18. **CACERES, R.A.**, TIMMERS, L.F.S.M., DIAS, R., BASSO, L.A., SANTOS, D.S., DE AZEVEDO, W.F. Molecular modeling and dynamics simulations of PNP from Streptococcus agalactiae. Bioorganic & Medicinal Chemistry. , v.16, p.4984 - 4993, 2008.

19. **CACERES, R.A.**, TIMMERS, L.F.S.M., VIVAN, A.L., SCHNEIDER, C.Z., BASSO, L.A., DE AZEVEDO, W.F., SANTOS, D.S. Molecular modeling and dynamics studies of cytidylate kinase from Mycobacterium tuberculosis H37Rv. Journal of Molecular Modeling. , v.14, p.427 - 434, 2008.

20. PAULI, I., **CACERES, R.A.**, DE AZEVEDO, W.F. Molecular modeling and dynamics studies of Shikimate kinase from Bacillus anthracis. Bioorganic & Medicinal Chemistry. , v.16, p.8098 - 8108, 2008.

21. BARCELLOS, G.B., PAULI, I., **CACERES, R.A.**, TIMMERS, L.F.S.M., DIAS, R., DE AZEVEDO, W.F.
Molecular Modeling as a Tool for Drug Discovery. Current Drug Targets. , v.9, p.1084 - 1091, 2008.

22. **CACERES, R.A.**, PAULI, I., TIMMERS, L.F.S.M., DE AZEVEDO, W.F. Molecular Recognition Models: A Challenge to Overcome. Current Drug Targets. , v.9, p.1077 - 1083, 2008.

23. TIMMERS, L.F.S.M., **CACERES, R.A.**, BASSO, L. A., SANTOS, D.S., DE AZEVEDO, W.F. Structural Bioinformatics Study of PNP from Listeria monocytogenes. Protein and Peptide Letters. , v.15, p.843 - 849, 2008.

24. TIMMERS, L.F.S.M., **CACERES, R.A.**, VIVAN, A.L., GAVA, L.M., DIAS, R., DUCATI, R.G., BASSO, L.A., SANTOS, D.S., DE AZEVEDO, W.F. Structural studies of human purine nucleoside phosphorylase: Towards a new specific empirical scoring function. Archives of Biochemistry and Biophysics. , v.479, p.28 - 38, 2008.

25. VIVAN, A.L., **CACERES, R.A.**, BELTRANO, J.R.A., BORGES, J.C., RUGGIERO NETO, J., RAMOS, C.H.I., DE AZEVEDO, W.F., BASSO, L. A., SANTOS, D.S. Structural studies of prephenate dehydratase from Mycobacterium tuberculosis H37Rv by SAXS, ultracentrifugation, and computational analysis. Proteins. , v.1, p.1352 - 1362, 2008.